



Published in final edited form as:

Tetrahedron. 2018 June 28; 74(26): 3358–3369. doi:10.1016/j.tet.2018.03.045.

Synthesis and Study of the Antimalarial Cardamom Peroxide

Xirui Hu^a, Pharath Lim^{b,c,d}, Rick M. Fairhurst^b, and Thomas J. Maimone^a

^aDepartment of Chemistry, University of California–Berkeley, Berkeley, CA 94720 (USA)

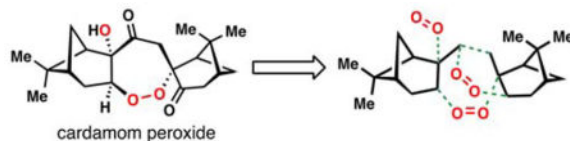
^bLaboratory of Malaria and Vector Research, National Institute of Allergy and Infectious Diseases, National Institutes of Health, Rockville, MD (USA)

^cNational Center for Parasitology, Entomology, and Malaria Control, Phnom Penh, Cambodia

Abstract

A full account of our previously disclosed synthesis of the monoterpene dimer cardamom peroxide is reported. Inspired by hypotheses regarding the potential biosynthetic origins of this natural product, several unproductive routes are also reported. The chemical reactivity of this structurally unique metabolite in the presence of iron(II) sources is also reported as is its antimalarial activity against *Plasmodium falciparum* clinical isolates from several Cambodian provinces.

Graphical Abstract



Keywords

malaria; endoperoxide; total synthesis; natural product

1. Introduction

Malaria, a parasitic disease transmitted by *Anopheles* mosquitoes, is prevalent in over 99 countries. More than 3 billion people are at risk of acquiring this disease worldwide, and an estimated 445,000 deaths occurred as a result of malaria in 2016.¹ Among the five known *Plasmodium* parasites that cause malaria in humans, *Plasmodium falciparum* is associated with the greatest mortality. Humanity's fight against malaria dates back to the 1600s, when Peruvian Indians were observed chewing on Cinchona bark to stop shivering.² The Cinchona bark, from which the early antimalarial drug quinine was isolated, was introduced into Europe as a treatment for malaria in the early 17th century.³ Driven by the needs of the military and the colonial powers, antimalarial drug development grew rapidly in the 20th century. Due to this demand, chloroquine was developed in 1934 and quickly became the front-line antimalarial drug after approval in 1946; however, a development of chloroquine

^dcurrent address: Medical Care Development International, Silver Spring, MD (USA)

resistance in parasites was observed.⁴ Sulfadoxine-pyrimethamine (SP), a combination of antifolates, served briefly as the successor of chloroquine, but widespread resistance to this substance also emerged after a period of only 5 years. In 1972, Tu and coworkers discovered the terpenoid peroxide artemisinin (**2**) from the leaves of *Artemisia annua*,⁵ a plant used for at least 2000 years for the treatment of fever by Chinese herbal medicine practitioners. Since then, artemisinin derivatives and artemisinin combination therapies (ACTs) have served as the front-line treatment for uncomplicated and severe *P. falciparum* infections. In the past decade however, continually growing reports detailing resistance to derivatives of **2** have surfaced, observations which severely threaten global malaria control.⁶

Since the isolation of **2** in the 1970's, a large number of endoperoxide-containing natural products of both terpenoid and polyketide origin have been discovered (Figure 1A).⁷ While far from approaching the remarkable low nM potency of **2** and its congeners, many of these compounds possess significant antimalarial activity and have thus proven to be attractive targets for chemical synthesis and the development of peroxidation methodology.^{8,9} Moreover, these naturally occurring O–O bond-containing molecules have also inspired the development of new synthetic antimalarials such as the ozonide arterolane and the endoperoxide arteflene which is based on the yingzhaosu A scaffold (Figure 1B).^{10,11}

Cardamom peroxide (**1**), a structurally interesting terpene endoperoxide was isolated in 1995 by Clardy and coworkers from *Amomum krevanh* fruit (Siam cardamom) (Figure 1).¹² Initial *in vitro* assays indicated that **1** exhibited strong inhibition of *P. falciparum* ($EC_{50} = 170$ nM), a potency similar to the synthetic antimalarial arteflene. Cardamom peroxide contains a rare seven-membered endoperoxide motif (1,2-dioxepane) thus making it an architecturally and biologically intriguing synthetic target. This feature combined with interest over its possible biosynthetic origins led us to target **1** for chemical synthesis. In 2014, we reported a 4-step synthesis of this natural product using oxygen as the sole sources of all of the oxygen atoms.¹³ Herein we provide a full account of our synthetic studies and further antimalarial evaluation of **1** against *P. falciparum* clinical isolates from several regions of Cambodia.

Retrosynthetically, we envisioned that **1** might be produced first in nature as diperoxide **3** and then chemoselectively reduced (Figure 2A). We viewed **3** as the result of a 7-*endo-trig* cyclization of either a peroxy radical or peroxide precursor (see **4**) followed by oxygenation of the resulting α -keto radical or enolate respectively. Enone **4** in turn could come from an air oxidation process of diketone **5**, which appears to be the product of a pinane-type monoterpene dimerization. We suspected that from **5**, the ketone α -oxygenation event and the 7-*endo* cyclization/oxygenation cascade would occur diastereoselectively as a result of the steric constraints placed by the pinane units. Thus it was our belief that enzymatic assistance would not be needed to dictate the stereochemical course of this reaction. Given that various monoterpenes were isolated alongside **1**, and the observation that the peroxide-forming step in the biosynthesis of **2** is non-enzymatic give credence to these ideas.^{12, 14} Nevertheless literature precedent suggested that the 7-*endo* cyclization would be challenging and we were cognizant that Mayrargue and coworkers could not forge the 1,2-dioxepane unit (see **7**) from pinene-derived model peroxide **6** via a radical cyclization that was competent in forging 1,2-dioxolane and 1,2-dioxane structures (Figure 2B).¹⁵

2. Results and Discussion

2.1. First generation attempt towards the synthesis of (+)-cardamom peroxide

Initial forays into the construction of the cardamom peroxide began with attempts to construct dimeric pinane-derived diketone **5** from the terpene chiral pool (Scheme 1).¹⁶ A Stetter-type coupling between enone **9**, prepared from pinene via intermediate peroxide **8**,¹⁷ and (–)-myrtenal proved unsuccessful under the mediation of thiazolium salt **10** and base. Also examined, but found to be unworkable, were the coupling of **9** and (–)-myrtenal either by Rh-catalyzed hydroacylation or SmI₂-mediated reductive coupling (Scheme 1A).^{18,19} While bromopinene **11** could be dimerized under reductive, titanocene-mediated conditions to give **12** (a plausible biogenetic precursor to **1**),²⁰ achieving the desired oxidation patterns found in **5** proved challenging (Scheme 1B). Initial success in forging **5** was eventually found via the pathway shown in Scheme 1C. First, a Cu(I)-mediated addition of the Grignard reagent prepared from **11** to enone **9** delivered 1,4-addition product **13** in 48% yield and as a single isomer after acidic work-up.²¹ Next, this material underwent allylic oxidation using selenium dioxide to form an allylic alcohol which was immediately oxidized with DMP. While this route provided the first glimpse of **5**, the very low yield encountered in the SeO₂ oxidation (12%, unoptimized) was a bottleneck for material throughput.

Concurrent with these studies, however, we discovered a superior route to **5** based on the chemistry shown in Scheme 1D. We opted to immediately dimerize (–)-myrtenal under reductive coupling conditions, a maneuver which produced triene **14** with more appropriately placed “handles” for further synthetic manipulation. While ultimately capable of providing gram quantities of material, this transformation required significant optimization under rigorously air- and moisture-free conditions (Table 1). While reductive coupling methods based on aluminum²² and chromium²³ failed to produce triene **14** (entries 1 and 2), several titanium reagents were applicable to this coupling. Conditions employing titanium powder as reductant produced a small amount of **14** with a variety of inseparable non-polar side products (entry 3).²⁴ Employing stoichiometric quantities of titanocene dichloride with added reducing agent successfully produced **14** as a single isomer (entries 4 and 5); however the catalytic version of this system failed to produce the desired product (entry 6).²⁵ The use of titanium tetrachloride, instead of Cp₂TiCl₂/reductant, favorably improved the yield to 35% (entry 7).²⁶ Synthetically useful yields (51% isolated) were obtained when the classic McMurry coupling procedure [TiCl₃, Zn-Cu alloy] was employed (entry 8).²⁷ This protocol also featured an easier workup protocol without the need for cumbersome removal of titanocene side products. However, due to the high cost of titanium (III) trichloride, this protocol was not directly applied in our synthesis, but slightly modified by using less expensive titanium (IV) tetrachloride and higher equivalents of the metal reductant (entry 9). Satisfyingly, the modified procedure offered an improved yield (62%) on small scale, and could be reproducibly performed on 3-gram scales in 53% yield. It should be noted that **14** proved to be quite unstable, decomposing to complex mixtures via both air oxidation as well as treatment with mildly acidic CDCl₃.

With **14** available in substantial quantities, efforts to install the two oxygens found in **5** were initiated (Scheme 1D). A [4+2] cycloaddition with singlet oxygen constructed endoperoxide

15, thus desymmetrizing C_2 -symmetric dimer **14**. Without isolation, this material was subject to Kornblum-DeLaMare fragmentation conditions (DBU) thus furnishing dienone **16**.^{28,29} We envisioned that a redox-neutral isomerization consisting of a γ -deprotonation/protonation sequence could forge **5** directly from **16**.³⁰ After examining a variety of conditions, some of which are noted in Scheme 1D, we found that simply stirring **16** with DBU in DCM cleanly-forged **5** within hours at room temperature. We also noted that after three days of prolonged stirring, **5** converted to a 3:1 mixture favoring diastereomer **17**, wherein the side chain has epimerized to relieve steric clash with the *gem*-dimethyl group of the neighboring pinane ring. With sufficient amounts of **5** and **17** in hand, we were poised to investigate the proposed tandem peroxidation cascade. Both isomers were then reacted under standard conditions known to elicit ketone α -peroxidation (*t*-BuOK, O₂).^{31–37} Unfortunately, we were unable to isolate any of diperoxide **3**; the major product isolated under these conditions was determined to be epoxide **18**. These findings led us to speculate that either anion **4** does not undergo an anionic 7-*endo* cyclization at a rate comparable to epoxide formation *or* that the α -peroxidation occurs at the undesired carbonyl first and then forms the epoxide.³⁸ This former hypothesis is somewhat corroborated by our later findings (see Figure 6), wherein we suspect that protonated **4** favors the formation of a peroxy hemiketal intermediate (see **25**) instead of undergoing the 7-*endo* cyclization. While ultimately unsuccessful, this work led us to consider alternative ways of generating radical **4**.

2.2. Total synthesis of (+)-cardamom peroxide

Our successful route to **3** (and ultimately **1**) commenced with previously prepared dienone alcohol **16** (Scheme 2A). Rather than isomerize this material, we oxidized it to dienone **19** with Dess-Martin periodinane. Alternatively, we also discovered a one-pot method to construct this material from **14** wherein the initial single oxygen [4+2] adduct (*i.e.* **15**) was treated with catalytic Co(II)-salen (**20**) according to Taylor's conditions (Scheme 2B).³⁹ This induced single-electron reduction of the endoperoxide, presumably generating radical **21** which undergoes 1,5-hydrogen atom abstraction to form ketone **22** and regenerate the Co^{II} complex. Enone **22** formed in this process, which is isomeric to **16**, could be oxidized in the same flask to directly deliver **19** in 72% overall yield from **14**.

With a sufficient amount of **19** in hand, extensive studies and optimization were necessary to realize the tandem radical hydroperoxidation reaction (**19** \rightarrow **3** or **1**). We recognized that if a hydrogen atom transfer (HAT), or alternatively a hydrometallation/homolytic M–C cleavage event, occurred in a regio- and chemoselective fashion onto **19**, intermediate **4** could be generated via diastereoselective reaction of an α -keto radical with ³O₂. This reaction requires the formal addition of the hydrogen atom to occur at the more electron-deficient alkene, a process we felt could be tuned via the metal-hydride generating precursor.⁴⁰ In addition, we felt the steric encombrance provided by the neighboring pinane ring could dictate the regioselectivity as well.

Our initial screening of metal precatalysts for this tandem peroxidation reaction began with several reported hydration/hydroperoxidation conditions (Table 2). In a pioneering 1989 study, Mukaiyama and Isayama achieved hydroperoxidation and hydration of electron-rich alkenes catalyzed by Co(acac)₂ and employing a mild silane reductant under an oxygen

atmosphere.⁴¹ In this work the authors reported that electron-deficient olefins, such as α,β -unsaturated esters, were not reactive to the cobalt-catalyzed system. This limitation was successfully resolved later by the same group in 1990,⁴² by replacing $\text{Co}(\text{acac})_2$ with a catalytic amount of bis(dipivaloylmethanato)-manganese(II) ($\text{Mn}(\text{dpm})_2$).⁴³ In 2000, Magnus and coworkers further investigated the manganese-catalyzed system, and extended the substrate scope to α,β -unsaturated ketones⁴⁴ and nitriles.⁴⁵ Interestingly, 1,4-reduction of enones⁴⁶ and reduction of ketones⁴⁷ were achieved under oxygen-free conditions with the same catalyst/reductant combination. Similar conditions were also recently extended to unactivated olefin reduction.^{48,49} In addition, iron-catalyzed hydroperoxidation and hydrations have been investigated by Kasuga⁵⁰ and Boger,^{51,52} utilizing iron(II) phthalocyanine [$\text{Fe}^{\text{II}}(\text{PC})$] and iron(III) oxalate [$\text{Fe}_2(\text{ox})_3$] in the presence of a strong reductant and oxygen.

As shown in Table 2, iron-based systems proved ineffective for the conversion **19**→**1** (Entries 1–3). The combination of iron oxalate and NaBH_4 appeared unreactive to enone **19** (entry 1), while conditions utilizing $\text{Fe}^{\text{II}}(\text{PC})$ and NaBH_4 proved highly reactive (entry 2). In the latter case, complete consumption of the starting material was observed after 15 minutes, and a complex mixture of products was obtained, among which the major product was identified as the monoterpene derivative nopinone (39%, GC yield). Under conditions employing $\text{Fe}(\text{acac})_3$ and PhSiH_3 (entry 3),⁵³ bisenone **19** did not react at low temperature, and therefore the reaction mixture was warmed to room temperature. Complete consumption of starting material was achieved after 16 hours; however **1** was not formed and significant quantities of nopinone were again detected.

To our delight, **1** was isolated in the cobalt- and manganese-catalyzed reactions after reductive workup in 6% and 34% yield, respectively (entries 4 and 5, Table 2). This finding is in accordance with the aforementioned superiority of manganese catalysts for functionalizing electron-deficient olefins.^{44–47} We next decided to evaluate other reaction parameters. It was discovered that the product composition of this tandem reaction was highly dependent on the concentration of oxygen relative to reductant. Decreasing the ratio of reductant to oxygen by slow addition of phenylsilane as a solution in dichloromethane over 12 h increased the yield of **1** to 41% with far fewer side-products formed (entry 6). Addition of *tert*-butyl hydroperoxide (TBHP) further increased the yield to 52% (entry 7), presumably due to faster oxidation of the $\text{Mn}(\text{dpm})_2$ intermediate back to a functional Mn(III) catalyst, a process that would consume molecular oxygen otherwise. Under our optimized conditions (entry 7), nopinone, hydration product **23**, and diol **24** side products were isolated in 9%, 11%, and 13% yields respectively. Synthetic cardamom peroxide (**1**) synthesized from (–)-myrtenal displayed $[\alpha]_{\text{D}} = +123.2^\circ$ ($c = 0.005$ g/mL, hexanes), which is in agreement with the reported value of $[\alpha]_{\text{D}} = +111.35^\circ$ (concentration not reported). The absolute configuration of synthetic **1** was unambiguously determined by X-ray analysis, and is opposite to that previously speculated by Clardy and coworkers.¹² Taking the one-pot transformation of **14** to **19** into account, the entire synthesis of **1** requires only three-steps.

2.3. Mechanistic studies of the tandem peroxidation reaction

Intrigued by the formation of nopinone and other byproducts formed in our key tandem peroxidation reaction, we sought to better understand the mechanisms by which these compounds may be formed (Figures 3 and 4). In a key experiment, we performed the reaction **19**→**1** using stoichiometric amounts of Mn(dpm)₃ and adding PhSiH₃ in a single portion (Figure 3). Under these non-catalytic conditions, **19** was consumed in less than ten minutes and only a small amount of diperoxide **3** was detected. Notably, a significant quantity of a mystery product tentatively assigned as peroxyketal **25**, which was both unstable and existed as a mixture of two diastereomers as determined by ¹H NMR spectroscopy, was detected under these conditions. Upon addition of triphenylphosphine to the crude reaction mixture, **25** and **3** were consumed and hydration product **23** and **1** could be isolated in yields of 40% and 9% respectively. Resubjecting the isolated hydration product **23** to the reaction conditions gave diol **24** in moderate yield and without the formation of nopinone. The same maneuver was then employed on a rapidly isolated sample of **25** (as an isomeric mixture). In this case we detected substantial amounts of nopinone, diol **24**, and a variety of decomposition products. We hypothesize that with sufficient molecular oxygen in solution and a reduced concentration of silane, the proposed peroxyradical intermediate (see **4**) is mainly funneled to diperoxyradical **26** which is the precursor to **3** (Figure 4). If, however, **4** is reduced too quickly, peroxyketal **25** is generated, thus triggering the formation of the downstream side-products nopinone, **23**, and **24**, presumably via **27** and **29**. The cleavage pathway from **27** to nopinone may proceed by the well-documented β-hydroxy hydroperoxide fragmentation reaction.^{54,55} If our hypothesis is correct, this pathway should also produce peroxy ester **28** as a byproduct, a compound we have not isolated to date. We have, however, observed small amounts (~5%) of dione **30**⁵⁶ in reactions utilizing the Co(acac)₂/PhSiH₃ system, conditions which also produce nopinone (Table 2, entry 4). It is plausible this compound comes from reduction of **28** with concomitant loss of acetic acid, a process likely driven by relief of steric strain with the *gem*-dimethyl group of the pinane ring system. While we *have not* isolated **30** from reactions employing the Mn(dpm)₃/PhSiH₃ system, we found that subjecting isolated **30** to these conditions elicits rapid decomposition, possibly via enol **31**, a species which could in principle undergo further hydroperoxidation chemistry. These findings suggest a reason why **28** and **30** evade detection under manganese-based conditions.

2.4 Reductive activation of (+)-cardamom peroxide

Despite longstanding and ongoing debate over the mechanism of action of **2** and antimalarial peroxides,⁵⁷ a pathway involving iron-induced peroxide O–O bond cleavage has been largely attributed as a key component contributing to their antimalarial activity; many associated mechanistic studies have been reported.^{58–61} Upon activation by a one-electron reduction, organic peroxides cleave to produce a metal alkoxide and an oxygen-centered radical through O–O bond cleavage, the latter of which initiates various downstream processes, including radical β-scission. These processes consequently generate carbon-centered radicals, carbocations, or epoxides depending on the structural properties of parent peroxide.⁶² In the case of **2**, primary alkyl radical **32** is formed, while arteflene and arterolane generate the secondary radicals shown (Figure 5). In order to examine the

reductive activation mode of **1**, we treated it with iron(II) chloride in a water/acetonitrile mixture under deoxygenated conditions (Figure 6A). Upon addition of the iron salt, a rapid solution color change of yellow/green to red was observed. After **1** was consumed, as judged by TLC, three major products vinylogous acid **36**, pyranone **37**, and furanone **38**, were isolated in yields of 20 %, 5–10 %, and 42 % respectively. The structure of **37** and **38** were confirmed by X-ray crystallographic analysis. Presumably, iron(II) chloride approaches the peroxide from the less-hindered side and leads to an oxygen-centered radical **33** that selectively cleaves the neighboring carbon-carbonyl bond. Oxidation of the resulting acyl radical **34** by the iron(III) center would generate acylium ion **35**, which upon addition of water forges the carboxylic acid moiety found in **36–38**. Pyranone **37** and furanone **38** are then formed via additional dehydrative cyclizations. According to the heme alkylation model for artemisinin bioactivity, primary radical **32** forms a covalent C–C bond with heme thus inhibiting hemozoin formation.⁶³ We viewed **34** or **35** as species also capable of undergoing a similar reaction and thus a biologically relevant reaction was conducted by treating cardamom peroxide (**1**) with heme dimethyl ester and the intracellular reductant glutathione (Figure 6B).⁶¹ We observed the formation of **38** along with three major, presumed porphyrin-containing adducts as judged by thin layer chromatography. Work-up and column chromatography yielded fractions with masses corresponding to heme/**1** adducts (see **39**, $m/z = 974.3963$, $C_{56}H_{62}FeN_4O_8$). Unfortunately to date, attempts to demetallate these complexes for NMR characterization have led only to decomposition. In addition, we have been unable to grow single crystals of **39** for X-ray diffraction studies. We stress that the structure of **39**, both with respect to the porphyrin attachment point, as well as the identity of the cardamom peroxide fragment attached, is not known. **39** represents a tentative structure and our data simply implies that the two pieces have joined.

2.5 Antimalarial evaluation of the cardamom peroxide

Recent reports of increased ACT failure rates have surfaced in western Cambodia,⁶ historically an epicenter for antimalarial drug resistance. A recent study surveyed drug susceptibilities of a variety of commonly used antimalarials (artesunate, DHA, quinine, piperazine, chloroquine, and mefloquine) against patient-derived *P. falciparum* isolates from three geographically distinct provinces of Cambodia: Ratanakiri (eastern region), Preah Vihear (central), and Pursat (western) (Figure 7).⁶⁴ With the exception of piperazine at the time, a general trend toward reduced sensitivity in clinical isolates derived from Pursat was noted. Evaluation of **1** against isolates from these regions is shown in Figure 7, with mean IC_{50} s of 613.3, 502.7, and 339.0 nM for Pursat, Preah Vihear, and Ratanakiri, respectively. It is worth noting that while **1** has not been used clinically, it shows a similar trend with western Cambodian field isolates being the least sensitive to its effects.^{65,66}

3. Conclusion

In conclusion, we have developed a practical synthesis of the antimalarial cardamom peroxide in as little as three steps and without recourse to the use of protecting groups.⁶⁷ While the antimalarial activity of **1** proved insufficient for further clinical consideration, a variety of interesting chemical findings were unearthed during our synthetic studies concerning both the potential origins of this natural product and its reactivity in comparison

to related and previously studied endoperoxides. The ability to construct highly oxygenated terpenes from molecular oxygen and simple, unfunctionalized terpene fragments holds much promise for streamlining the chemical synthesis of other complex natural products. Efforts to extend this concept to other complex problems in synthesis are underway and will be reported in due course.

4. Experimental section

4.1 General

Dry tetrahydrofuran (THF), dichloromethane (DCM), toluene, hexane, acetonitrile, and diethyl ether were obtained by passing these previously degassed solvents through activated alumina columns. Amines and alcohols were distilled from calcium hydride prior to use. 1,2-Dimethoxyethane (DME) was distilled from sodium and benzophenone. TiCl_4 was distilled prior to use. (-)-Pinene, (-)-myrtenol, and (-)-myrtenal was purchased from Sigma Aldrich and used directly without further purification. Reactions were monitored by thin layer chromatography (TLC) on Silicycle Siliaplate™ G TLC plates (250 μm thickness, 60 \AA porosity, F-254 indicator) and visualized by UV irradiation and staining with *p*-anisaldehyde or potassium permanganate developing agents. Volatile solvents were removed under reduced pressure using a rotary evaporator. Flash column chromatography was performed using Silicycle F60 silica gel (60 \AA , 230–400 mesh, 40–63 μm). Proton nuclear magnetic resonance (^1H NMR) and carbon nuclear magnetic resonance (^{13}C NMR) spectra were recorded on Bruker AV-300, AVB-400, AV-500, or AV-600 spectrometers operating respectively at 300, 400, 500, and 600 MHz for ^1H , and 75, 100, 125, and 150 MHz for ^{13}C . Chemical shifts are reported in parts per million (ppm) with respect to the residual solvent signal CDCl_3 (^1H NMR: $\delta = 7.26$; ^{13}C NMR: $\delta = 77.16$). Peak multiplicities are reported as follows: s = singlet, bs = broad singlet, d = doublet, t = triplet, dd = doublet of doublets, td = triplet of doublets, m = multiplet. app = apparent. Melting points were determined using MEI-TEMP™ apparatus and are uncorrected. IR spectra were recorded on a Nicolet 380 FT-IR spectrometer. High-resolution mass spectra (HRMS) were obtained by the qb3 mass spectrometry facility at the University of California, Berkeley (a VG Prospec Micromass spectrometer for EI). Optical rotations were measured on a Perkin-Elmer 241 polarimeter. X-ray crystallographic analyses were performed at the UC Berkeley College of Chemistry X-ray crystallography facility.

4.2 Experimental procedures and data for synthetic compounds

4.2.1. Ketone 13—The procedure was adapted from previous conditions reported by Lipshutz and co-workers (*J. Org. Chem.* **1994**, *59*, 7437.) A flame-dried 100 mL round-bottom flask was charged with Mg^0 turnings (1.25 g) and THF (5 mL). A drop of dibromoethane was added at 0 $^\circ\text{C}$ followed by a solution of bromide **11** (0.50 g, 2.5 mmol) in THF (5 mL) added dropwise over 2 hours at -13 $^\circ\text{C}$. The reaction was then warmed to room temperature and stirred for an additional 30 minutes. The resulting grey solution was transferred to a separate round-bottom flask pre-charged with CuI (0.524 g, 2.75 mmol), Me_2S (0.5 mL, 13.75 mmol), dry LiCl (117 mg, 2.75 mmol) and THF (5 mL) at -78 $^\circ\text{C}$. The resulting mixture was stirred for 10 minutes, followed by the addition of TMSCl (0.35 mL, 2.75 mmol) and enone **9** (0.30 g, 2 mmol). The reaction was monitored by TLC

analysis, and was quenched by the addition of saturated *aq.* NH₄Cl (5 mL) after the complete consumption of **9**. The resulting mixture was extracted by EtOAc and washed with brine. Column Chromatography (EtOAc/hexanes 1:20) gave ketone **13** (0.27 g, 48% yield) as a colorless oil: R_f=0.28 (DCM:hexane 1:2); ¹H NMR (300 MHz, CDCl₃) δ 5.18 (ddd, J = 3.0, 3.0, 1.5 Hz, 1H), 2.69 – 2.56 (m, 2H), 2.50 (dd, J = 19.3, 2.4 Hz, 1H), 2.34 (ddd, J = 8.5, 5.6, 5.6 Hz, 1H), 2.29 – 1.90 (m, 11H), 1.31 (s, 3H), 1.26 (s, 3H), 1.12 (m, 2H), 0.85 (s, 3H), 0.80 (s, 3H); ¹³C NMR (75 MHz, CDCl₃) δ 214.8, 147.9, 116.5, 56.5, 45.8, 44.9, 41.9, 41.0, 39.3, 38.8, 38.1, 35.4, 34.1, 31.8, 31.4, 28.7, 27.2, 26.5, 22.2, 21.3.

4.2.2. Keto-enone 5 (and 17)—[Procedure 1] A flame-dried 25 mL round-bottom flask was charged with ketone **13** (270 mg, 0.95 mmol), 2-hydroxybenzoic acid (14.0 mg, 0.1 mmol), and DCM (5 mL). SeO₂ (11.0 mg, 0.1 mmol) and TBHP (0.57 mL, 3.4 mmol, 6M in decane) was added sequentially. The reaction mixture was stirred at room temperature for 3 days and then quenched by the addition of saturated *aq.* Na₂S₂O₃ (2 mL). The resulting mixture was extracted by DCM and washed with brine. Flash column chromatography afforded the allylic alcohol product (33.0 mg, 0.11 mmol). The alcohol was then dissolved in DCM (1.1 mL) and DMP (56 mg, 0.132 mmol) and NaHCO₃ (10 mg, 0.11 mmol) were added sequentially. The reaction was monitored by TLC for consumption of starting material, quenched by the addition of brine, extracted with EtOAc, dried over Na₂SO₄, and concentrated *in vacuo*. Flash column chromatography gave **5** (30.0 mg, 11% yield from **13**) as a colorless oil: ¹H NMR (500 MHz, CDCl₃) δ 6.76 (dddd, J = 3.2, 3.2, 1.5, 1.5 Hz, 1H), 3.47 (dd, J = 16.9, 3.4 Hz, 1H), 3.12 – 3.08 (m, 1H), 2.93 (ddd, J = 5.6, 5.6, 1.6 Hz, 1H), 2.70 – 2.61 (m, 2H), 2.60 – 2.54 (m, 1H), 2.54 (dd, J = 16.9, 9.1 Hz, 1H), 2.50 (ddd, J = 19.9, 3.2, 3.2 Hz, 1H), 2.47 – 2.41 (m, 2H), 2.15 – 2.11 (m, 2H), 2.09 (ddd, J = 6.2, 6.2, 2.0 Hz, 1H), 1.32 (s, 3H), 1.30 (d, J = 10.6 Hz, 1H), 1.29 (s, 3H), 1.03 (d, J = 9.1 Hz, 1H), 0.88 (s, 3H), 0.74 (s, 3H); ¹³C NMR (125 MHz, CDCl₃) δ 214.0, 197.2, 149.1, 137.0, 52.3, 44.9, 43.3, 40.4, 39.8, 39.8, 39.1, 38.9, 37.6, 34.5, 32.7, 31.3, 26.9, 26.0, 22.2, 21.0. IR (thin film, cm⁻¹) 2922, 1714, 1666, 1615, 1468, 1410, 1369; HRMS (EI) calcd. for [C₂₀H₂₈O₂]: *m/z* 300.2089, found 300.2089.

[Procedure 2] A flame-dried round-bottom flask was charged with DBU (0.6 ml, 3.67 mmol) and DCM (7.2 ml) and then degassed by bubbling a stream of argon through the solution for 20 min. The resulting mixture was added via cannula to a flame-dried round-bottom flask charged with **16** (110 mg, 0.367 mmol) under an argon atmosphere. The reaction mixture was stirred for 3 days at room temperature and then quenched with 1N HCl. The aqueous phase was extracted with DCM and the combined organic phase washed with saturated *aq.* NaHCO₃ and brine. Flash column chromatography (EtOAc/hexanes 1:20) gave recovered starting material (27 mg, 25 %), and **5** and **17** (60 mg, 55%, 1:3 *dr*) as a colorless oil. The diastereomeric ratio was determined by ¹H NMR: ¹H NMR (600 MHz, CDCl₃) δ 6.75 (dddd, J = 3.2, 3.2, 1.5, 1.5 Hz, 1H), 3.20 – 3.17 (m, 1H), 3.15 (dd, J = 16.3, 3.2 Hz, 1H), 2.92 (ddd, J = 5.7, 5.7, 1.6 Hz, 1H), 2.71 – 2.63 (m, 2H), 2.50 (ddd, J = 19.9, 3.2, 3.2 Hz, 1H), 2.48 – 2.40 (m, 4H), 2.15 – 2.10 (m, 2H), 1.96 (ddd, J = 6.2, 6.2, 2.1 Hz, 1H), 1.31 (s, 3H), 1.31 (s, 3H), 1.11 (d, J = 10.9 Hz, 1H), 1.03 (d, J = 9.2 Hz, 1H), 0.95 (s, 3H), 0.72 (s, 3H); ¹³C NMR (100 MHz, CDCl₃) δ 214.3, 197.3, 149.3, 137.0, 48.7, 44.6, 42.3, 40.4, 39.9, 39.5, 38.3, 37.4, 36.9, 32.7, 31.2, 29.4, 26.4, 26.0, 21.0, 20.0.

4.2.3. Epoxide 18—A flame-dried round-bottom flask was charged with **5** and **17** (30 mg, 0.1 mmol, mixture of two diastereomers), THF (4 ml) and *tert*-butanol (1 ml). The resulting solution was cooled to $-40\text{ }^{\circ}\text{C}$ and oxygen was bubbled through the solution for 10 minutes. Potassium *tert*-butoxide (45 mg, 0.4 mmol) was then added as solid in one portion to the reaction. The reaction mixture was quenched after 30 minutes by the addition of 1N *aq.* HCl, extracted with DCM, and washed with brine. Column Chromatography (EtOAc/hexanes 1:15 to 1:10) gave recovered starting material, and **18** (11 mg, 35% yield) as a colorless oil: $[\alpha]_{\text{D}}^{20} +170.6^{\circ}$ (c 0.005 g/ml, CHCl_3); $^1\text{H NMR}$ (500 MHz, CDCl_3) δ 6.93 (dddd, $J = 3.1, 3.1, 1.4, 1.4$ Hz, 1H), 2.95 (ddd, $J = 5.7, 5.7, 1.6$ Hz, 1H), 2.78 – 2.62 (m, 3H), 2.52 – 2.50 (m, 2H), 2.47 (ddd, $J = 9.2, 5.7, 5.7$ Hz, 1H), 2.25 (dddd, $J = 6.1, 6.1, 2.9, 2.9$ Hz, 1H), 2.16 (dddd, $J = 5.7, 5.7, 2.8, 2.8$ Hz, 1H), 2.01 (dd, $J = 6.0, 6.0$ Hz, 1H), 1.58 (d, $J = 11.1$ Hz, 1H), 1.33 (s, 3H), 1.28 (s, 3H), 0.97 (d, $J = 9.2$ Hz, 1H), 0.85 (s, 3H), 0.77 (s, 3H); $^{13}\text{C NMR}$ (100 MHz, CDCl_3) δ 206.5, 189.8, 149.1, 140.8, 67.5, 61.5, 42.8, 40.5, 40.5, 40.4, 39.6, 38.2, 37.5, 33.1, 31.3, 29.9, 26.2, 25.9, 21.6, 21.1; IR (thin film, cm^{-1}) 2935, 1730, 1671, 1611, 1467, 1419, 1370, 1274; HRMS (EI) calcd. for $[\text{C}_{20}\text{H}_{26}\text{O}_3]$: m/z 314.1882, found 314.1885.

4.2.4. Triene 14—The procedure was adapted from previous conditions reported by McMurry and co-workers (*J. Org. Chem.* **1978**, *43*, 3255.) A flame-dried 1 L three-necked flask equipped with a large stir bar and reflux condenser was charged with freshly prepared Zn-Cu couple (44 g, 0.67 mol, 40 equiv). The system was evacuated and backfilled with argon three times. DME (600 mL) was added, followed by the dropwise addition of freshly distilled TiCl_4 (24 ml, 200 mmol, 10 equiv) to the rapidly stirring slurry. After 1 hour of sonication, the mixture was heated to reflux for 5 hours, cooled to room temperature, and a solution of myrtenal (3.0 g, 20 mmol, 1 equiv) in 50 mL of degassed DME was added slowly over 12 hours via syringe pump. After 1 hour of additional sonication, the reaction mixture was heated at reflux for 48 hours, cooled to room temperature, and filtered through a pad of Florisil® eluting with diethyl ether. This filtration was repeated to give a clear solution that was concentrated *in vacuo* and purified by flash column chromatography (200:1 hexanes: Et_3N) to afford **14** (1.41 g, 53 % yield) as a colorless oil: $[\alpha]_{\text{D}}^{20} = +31.70^{\circ}$ (c 0.010 g/ml, CHCl_3); $^1\text{H NMR}$ (500 MHz, CDCl_3) δ 6.14 (s, 2H), 5.53 (m, 2H), 2.62 (ddd, $J = 5.7, 5.7, 1.6$ Hz, 2H), 2.42 (ddd, $J = 8.8, 5.7, 5.7$ Hz, 2H), 2.39 (ddd, $J = 19.2, 3.0, 3.0$ Hz, 2H), 2.32 (ddd, $J = 19.2, 2.7, 2.7$ Hz, 2H), 2.12 (m, 2H), 1.33 (s, 6H), 1.13 (d, $J = 8.8$ Hz, 2H), 0.81 (s, 6H); $^{13}\text{C NMR}$ (150 MHz, CDCl_3) δ 146.9, 126.4, 123.7, 41.3, 41.2, 37.9, 32.2, 31.6, 26.6, 21.0; IR (thin film, cm^{-1}) 2931, 2360, 1705, 1650, 1628, 1369, 1331; HRMS (EI) calcd. for $[\text{C}_{20}\text{H}_{28}]$: m/z 268.2191, found 268.2191.

4.2.5. Dienone alcohol 16—A flame-dried round-bottom flask was charged with triene **14** (1.3 g, 4.84 mmol, 1 equiv) and DCM (145 ml). The solution was cooled to $-40\text{ }^{\circ}\text{C}$ and methylene blue (15 mg, 0.05 mmol, 0.01 equiv) in DCM (1 mL) was added. Oxygen gas was vigorously bubbled through the solution while irradiating with a 500 W halogen lamp. After 1 hour, a second portion of methylene blue (15 mg) in DCM (1 mL) was added and the irradiation was continued until TLC indicated complete consumption of the starting material (~2 hours). Nitrogen was then bubbled through the solution for 30 minutes at which point DBU (3.7 mL, 24 mmol, 5 equiv) was added dropwise at $-40\text{ }^{\circ}\text{C}$. The resulting mixture was

allowed to gradually warm to $-20\text{ }^{\circ}\text{C}$ and stirred for an additional 4 hours at this temperature. The reaction mixture was quenched by the addition of 1 N HCl and extracted with DCM. The combined organic layers were washed with *sat. aq.* NaHCO_3 , H_2O , brine, dried over MgSO_4 , and concentrated *in vacuo*. The crude material was purified by column chromatography (gradient 20:1 \rightarrow 10:1 hexanes/ethyl acetate) to afford **16** (816 mg, 56 %) as white solid: mp $118.4 - 119.6\text{ }^{\circ}\text{C}$; $[\alpha]_{\text{D}}^{20} = +246.02^{\circ}$ (c 0.005 g/ml, CHCl_3); ^1H NMR (500 MHz, CDCl_3) δ 6.76 (dddd, $J = 3.3, 3.3, 1.5, 1.5\text{ Hz}$, 1H), 6.40 (d, $J = 0.8\text{ Hz}$, 1H), 5.11 (d, $J = 3.0\text{ Hz}$, 1H, D_2O exchangeable), 4.66 – 4.62 (m, 1H), 2.94 (ddd, $J = 5.7, 5.7, 1.5\text{ Hz}$, 1H), 2.56 – 2.50 (m, 2H), 2.49 – 2.40 (m, 3H), 2.38 – 2.31 (m, 1H), 2.16 – 2.11 (m, 1H), 2.07 (dddd, $J = 6.0, 6.0, 6.0, 2.2\text{ Hz}$, 1H), 1.95 (dd, $J = 14.6, 3.6\text{ Hz}$, 1H), 1.72 (d, $J = 10.0\text{ Hz}$, 1H), 1.34 (s, 3H), 1.31 (s, 3H), 1.07 (d, $J = 9.2\text{ Hz}$, 1H), 0.75 (s, 3H), 0.69 (s, 3H); ^{13}C NMR (125 MHz, CDCl_3) δ 191.2, 168.3, 150.6, 137.3, 120.4, 62.9, 53.5, 40.8, 40.3, 40.2, 40.0, 37.5, 33.8, 32.7, 31.2, 27.4, 26.0, 25.9, 22.7, 21.0; IR (thin film, cm^{-1}) 3421, 2916, 1636, 1591, 1393, 1366; HRMS (EI) calcd. for $[\text{C}_{20}\text{H}_{28}\text{O}_2]$: m/z 300.2089, found 300.2094.

4.2.6. Bisenone 19—Dienone alcohol **16** (816 mg, 2.72 mmol, 1.0 equiv) was dissolved in DCM (27 mL) and NaHCO_3 (228 mg, 2.72 mmol, 1.0 equiv) and Dess-Martin periodinane (1.5 g, 3.54 mmol, 1.3 equiv) were added sequentially. The resulting mixture was stirred at room temperature for 1 h (monitored by TLC for complete consumption of **16**). The reaction mixture was quenched by the addition of 1 N *aq.* NaOH and extracted with DCM. The combined organic phases were washed with water and brine, dried over MgSO_4 , and purified by flash column chromatography (gradient 20:1 \rightarrow 10:1 hexanes/ethyl acetate), affording **19** (770 mg, 95 %) as white solid: mp $137.1 - 138.4\text{ }^{\circ}\text{C}$; $[\alpha]_{\text{D}}^{20} +27.20^{\circ}$ (c 0.005 g/ml, CHCl_3); ^1H NMR (500 MHz, CDCl_3) δ 6.55 (ddd, $J = 3.4, 1.8, 1.8\text{ Hz}$, 1H), 6.00 (s, 1H), 3.05 (dd, $J = 5.5, 5.5\text{ Hz}$, 1H), 2.77 – 2.68 (m, 2H), 2.64 (ddd, $J = 19.2, 2.4, 2.4\text{ Hz}$, 1H), 2.54 – 2.41 (m, 3H), 2.39 (ddd, $J = 19.9, 2.9, 2.9\text{ Hz}$, 1H), 2.21 (dddd, $J = 6.1, 6.1, 2.8, 2.8\text{ Hz}$, 1H), 2.15 – 2.10 (m, 1H), 1.42 (dd, $J = 2.9, 2.9\text{ Hz}$, 1H), 1.40 (s, 3H), 1.35 (s, 3H), 1.08 (d, $J = 9.1\text{ Hz}$, 1H), 0.91 (s, 3H), 0.81 (s, 3H); ^{13}C NMR (125 MHz, CDCl_3) δ 198.4, 195.0, 149.7, 145.0, 138.3, 132.8, 48.9, 42.6, 41.3, 40.8, 39.3, 38.4, 37.9, 32.7, 32.3, 31.2, 26.0, 26.0, 22.0, 21.0; IR (thin film, cm^{-1}) 2931, 1705, 1651, 1628, 1465, 1421, 1368; HRMS (EI) calcd. for $[\text{C}_{20}\text{H}_{26}\text{O}_2]$: m/z 298.1933, found 298.1937.

4.2.7. Cardamom peroxide (1), hydration product 23, and diol 24—A flame-dried round-bottom flask was charged with bisenone **19** (30 mg, 0.1 mmol, 1.0 equiv), $\text{Mn}(\text{dpm})_3$ (12 mg, 0.02 mmol, 20 mol %), DCM (1.6 mL), and *i*-PrOH (0.4 mL). Oxygen was vigorously bubbled through the solution for 5 minutes, followed by the addition of TBHP (5M in decane, 30 μL , 1.5 equiv). The solution was cooled to $-10\text{ }^{\circ}\text{C}$ under an atmosphere of oxygen, and PhSiH_3 (30 μL , 0.24 mmol, 2.4 equiv) in DCM (1 mL) was added dropwise over 12 h via syringe pump. After the addition was complete, a solution of triphenylphosphine (56 mg, 0.21 mmol) in DCM was added dropwise at $-10\text{ }^{\circ}\text{C}$ to quench the hydroperoxide intermediates. The reaction mixture was diluted with H_2O (5 mL) and extracted with DCM ($3 \times 10\text{ mL}$). The combined organic layers were washed with brine, dried over Na_2SO_4 , filtered through Celite®, and concentrated *in vacuo*. The crude mixture was purified by flash column chromatography (DCM) to afford **1** (18.2 mg, 52%) as a white solid, along with hydration product **23** (3.5 mg, 11%), diol **24** (4.4 mg, 13%), and nopinone

(9% GC yield using an internal standard of dodecane). [Note: the reaction afforded 48% of **1** on a 150 mg scale].

(+)-Cardamom peroxide (**1**): white solid: mp 154.9 – 156.2 °C; $[\alpha]_D^{20} +123.20^\circ$ (c 0.005 g/ml, hexanes); $^1\text{H NMR}$ (500 MHz, CDCl_3) δ 4.28 (s, 1H), 4.22 (d, $J = 11.3$ Hz, 1H), 4.18 (d, $J = 8.7$ Hz, 1H), 2.78 (dd, $J = 18.9, 2.4$ Hz, 1H), 2.69 (ddd, $J = 18.9, 3.0, 3.0$ Hz, 1H), 2.58 (dd, $J = 15.4, 8.9$ Hz, 1H), 2.46 (dddd, $J = 11.0, 5.8, 2.9, 2.9$ Hz, 2H), 2.40 (d, $J = 11.2$ Hz, 1H), 2.41 – 2.35 (m, 1H), 2.30 (dd, $J = 6.1, 6.1$ Hz, 1H), 2.15 – 2.05 (m, 2H), 1.97 – 1.92 (m, 1H), 1.84 – 1.74 (m, 2H), 1.69 (d, $J = 11.2$ Hz, 1H), 1.38 (s, 3H), 1.27 (s, 3H), 1.06 (s, 3H), 0.86 (s, 3H); $^{13}\text{C NMR}$ (100 MHz, CDCl_3) δ 208.8, 204.5, 84.3, 84.2, 83.3, 49.6, 43.9, 43.3, 42.9, 41.0, 40.7, 39.0, 38.3, 30.7, 27.9, 27.5, 26.9, 26.6, 24.1, 22.5; IR (thin film, cm^{-1}) 3447, 3021, 2909, 1722, 1692, 1441, 1406, 1371; HRMS (ESI) calcd. for $[\text{C}_{20}\text{H}_{28}\text{O}_5\text{Na}]^+$ ($\text{M}+\text{Na}$) $^+$: m/z 371.1829, found 371.1837. Vapor diffusion of an ether solution of **1** with pentane afforded X-ray quality crystals.

Hydration product **23**: colorless oil; $[\alpha]_D^{20} = -56.7^\circ$ (c 0.006 g/ml, CHCl_3); $^1\text{H NMR}$ (500 MHz, CDCl_3) δ 6.70 (ddd, $J = 3.4, 1.8, 1.8$ Hz, 1H), 3.38 (d, $J = 15.7$ Hz, 1H), 2.99 (ddd, $J = 5.7, 5.7, 1.6$ Hz, 1H), 2.68 (dd, $J = 19.0, 2.4$ Hz, 1H), 2.59 (ddd, $J = 19.0, 3.2, 3.2$ Hz, 1H), 2.53 (dt, $J = 20.2, 3.2, 3.2$ Hz, 1H), 2.50 – 2.41 (m, 3H), 2.39 (d, $J = 15.8$ Hz, 1H), 2.22 (dd, $J = 6.2, 6.2$ Hz, 1H), 2.15 (dddd, $J = 5.9, 3.0, 3.0, 1.2$ Hz, 1H), 2.11 (dddd, $J = 6.1, 6.1, 3.0, 3.0$ Hz, 1H), 1.92 (d, $J = 11.0$ Hz, 1H), 1.36 (s, 3H), 1.35 (s, 3H), 1.02 (d, $J = 9.1$ Hz, 1H), 0.95 (s, 3H), 0.82 (s, 3H); $^{13}\text{C NMR}$ (100 MHz, CDCl_3) δ 210.6, 200.6, 150.4, 138.8, 79.8, 50.0, 43.3, 40.4, 40.3, 39.6, 39.3, 38.6, 37.6, 32.9, 31.2, 27.9, 27.4, 26.0, 22.9, 21.0; IR (thin film, cm^{-1}) 3359, 2924, 1721, 1640, 1613, 1421, 1370; HRMS (EI) calcd. for $[\text{C}_{20}\text{H}_{28}\text{O}_3]$: m/z 316.2038, found 316.2040.

Diol **24**: white solid (acid sensitive): mp 132.9 – 134.1 °C; $[\alpha]_D^{20} -33.2^\circ$ (c 0.010 g/ml, CH_2Cl_2); $^1\text{H NMR}$ (600 MHz, CD_2Cl_2) δ 5.49 (s, 1H), 3.37 (d, $J = 15.3$ Hz, 1H), 2.78 (ddd, $J = 15.8, 10.5, 3.5$ Hz, 1H), 2.69 – 2.62 (m, 2H), 2.57 (ddd, $J = 19.1, 3.2, 3.2$ Hz, 1H), 2.41 (dddd, $J = 11.0, 6.2, 6.2, 3.1$ Hz, 1H), 2.26 (dddd, $J = 10.1, 6.0, 6.0, 1.8$ Hz, 1H), 2.21 (dd, $J = 6.1, 4.8$ Hz, 1H), 2.18 – 2.14 (m, 2H), 2.08 (dddd, $J = 6.1, 6.1, 2.9, 2.9$ Hz, 1H), 1.99 – 1.90 (m, 2H), 1.85 (d, $J = 10.9$ Hz, 1H), 1.87 – 1.81 (m, 1H), 1.61 (ddd, $J = 16.0, 11.0, 5.2$ Hz, 1H), 1.58 (d, $J = 10.1$ Hz, 1H), 1.35 (s, 3H), 1.22 (s, 3H), 0.90 (s, 3H), 0.72 (s, 3H); $^{13}\text{C NMR}$ (150 MHz, CD_2Cl_2) δ 213.2, 213.1, 82.5, 80.4, 50.7, 49.0, 43.6, 41.7, 41.1, 39.7, 39.0, 38.3, 28.0, 27.5, 27.3, 26.2, 24.6, 24.3, 22.8, 22.0; IR (thin film, cm^{-1}) 3410, 3005, 2925, 2360, 2341, 1823, 1708, 1463, 1408, 1326; HRMS (ESI) calcd. for $[\text{C}_{20}\text{H}_{30}\text{O}_4\text{Na}]^+$ ($\text{M}+\text{Na}$) $^+$: m/z 357.2036, found 357.2035.

4.2.8. Acid 36, pyranone 37, and furanone 38—In a nitrogen-filled glovebox, **1** (12 mg, 0.03 mmol, 1.0 equiv) was dissolved in thoroughly degassed acetonitrile (750 μL) and H_2O (7 μL , 0.4 mmol, 13.0 equiv). To the resulting solution was added FeCl_2 (3.5 mg, 0.028 mmol, 0.8 equiv) in one portion and the resulting mixture stirred for 45 minutes. After 45 minutes, the resulting red colored solution was removed from the glovebox, opened to the air, diluted with DCM (15 mL) and washed with brine (2×25 mL). The organic phase was concentrated *in vacuo* and the crude material purified by preparative thin layer

chromatography (50:6 DCM:MeOH) affording acids **36** (2.5 mg, yield 20 %), **38** (5 mg, yield 42%), and a small amount of **37** (~ 0.5 – 1.0 mg, yield 5 – 10 %).

Acid **36**: white foam (unstable over extended periods in CDCl_3 , converts to **37** and **38**); $[\alpha]_D^{20} +48.0^\circ$ (c 0.001 g/ml, CH_2Cl_2); $^1\text{H NMR}$ (600 MHz, CD_2Cl_2) δ 5.25 (d, $J = 0.8$ Hz, 1H), 4.48 – 4.40 (m, 1H), 2.98 (ddd, $J = 10.4, 7.6, 0.8$ Hz, 1H), 2.91 (d, $J = 11.0$ Hz, 1H), 2.83 (dd, $J = 18.1, 6.7$ Hz, 1H), 2.73 (dd, $J = 18.1, 7.9$ Hz, 1H), 2.73 – 2.68 (m, 1H), 2.50 – 2.43 (m, 1H), 2.26 (ddd, $J = 11.1, 7.9, 7.9$ Hz, 1H), 2.26 – 2.21 (m, 1H), 2.10 (d, $J = 11.2$ Hz, 1H), 2.02 – 1.96 (m, 2H), 1.80 – 1.69 (m, 2H), 1.26 (s, 3H), 1.24 (s, 3H), 1.02 (s, 3H), 0.89 (s, 3H); $^{13}\text{C NMR}$ (125 MHz, CD_2Cl_2) δ 206.0, 199.0, 192.8, 102.9, 96.7, 68.2, 50.3, 44.7, 43.9, 40.3, 40.0, 39.0, 38.0, 37.4, 30.6, 26.9, 25.8, 24.7, 23.7, 18.0; IR (thin film, cm^{-1}) 3061, 2926, 2349, 1724, 1598, 1548, 1484, 1379; HRMS (ESI) calcd. for $[\text{C}_{20}\text{H}_{27}\text{O}_5]^- (\text{M}-\text{H}_2\text{O}-\text{H})^-$: m/z 347.1864, found 347.1863.

Furanone **38**: white solid: mp 147.5 – 149.8 $^\circ\text{C}$; $[\alpha]_D^{20} +77.50^\circ$ (c 0.002 g/ml, CH_2Cl_2); $^1\text{H NMR}$ (600 MHz, CDCl_3) δ 5.30 (s, 1H), 4.50 (dd, $J = 9.7, 4.3$ Hz, 1H), 2.95 (dd, $J = 10.6, 7.7$ Hz, 1H), 2.73 (dddd, $J = 14.8, 9.8, 2.8, 2.8$ Hz, 1H), 2.49 (dddd, $J = 10.3, 7.8, 7.8, 7.7$ Hz, 1H), 2.43 (dd, $J = 15.8, 7.2$ Hz, 1H), 2.34 (dd, $J = 15.8, 8.0$ Hz, 1H), 2.30 (ddd, $J = 11.3, 7.8, 7.8$ Hz, 1H), 2.26 (dddd, $J = 11.9, 6.2, 3.0, 3.0, 2.3$ Hz, 1H), 2.15 (d, $J = 11.3$ Hz, 1H), 2.03 – 1.97 (m, 2H), 1.83 – 1.74 (m, 2H), 1.27 (s, 3H), 1.25 (s, 3H), 1.03 (s, 3H), 0.93 (s, 3H); $^{13}\text{C NMR}$ (125 MHz, CDCl_3) δ 206.0, 192.5, 176.9, 102.8, 96.5, 67.9, 50.0, 44.3, 43.4, 39.9, 39.5, 38.7, 38.6, 34.8, 30.4, 26.8, 25.5, 24.4, 23.6, 17.5; IR (thin film, cm^{-1}) 3849, 3105, 2997, 2924, 2361, 1682, 1587, 1484, 1368; HRMS (ESI) calcd. for $[\text{C}_{20}\text{H}_{27}\text{O}_5]^- (\text{M}-\text{H})^-$: m/z 347.1864, found 347.1861. Vapor diffusion of an ether solution of **38** with pentane afforded X-ray quality crystals.

Pyranone **37**: white solid: mp 154.3 – 156.0 $^\circ\text{C}$; $^1\text{H NMR}$ (600 MHz, CD_2Cl_2) δ 5.27 (s, 1H), 4.98 (dd, $J = 9.1, 3.9$ Hz, 1H), 2.77 – 2.71 (m, 1H), 2.71 (dd, $J = 10.8, 7.6$ Hz, 1H), 2.43 – 2.35 (m, 2H), 2.34 – 2.25 (m, 2H), 2.22 (dd, $J = 5.8, 5.8$ Hz, 1H), 2.14 (ddd, $J = 11.0, 7.5, 7.5$ Hz, 1H), 1.99 (dddd, $J = 5.7, 5.7, 3.3, 3.3$ Hz, 1H), 1.90 (ddd, $J = 14.6, 3.8, 3.8$ Hz, 1H), 1.79 (dd, $J = 10.6, 10.6$ Hz, 1H), 1.27 (s, 3H), 1.22 (s, 3H), 1.10 (ddd, $J = 6.1, 3.8, 3.8$ Hz, 1H), 1.05 (s, 3H), 0.95 (s, 3H); IR (thin film, cm^{-1}) 3457, 2997, 2923, 2667, 2365, 1677, 1591, 1367; HRMS (ESI) calcd. for $[\text{C}_{20}\text{H}_{27}\text{O}_5]^- (\text{M}-\text{H})^-$: m/z 347.1864, found 347.1863. Vapor diffusion of an ether solution of **37** with pentane afforded X-ray quality crystals.

4.2.9. Reaction of 1 with hemin dimethyl ester—In a nitrogen-filled glove box, a 20 mL vial was charged with hemin dimethyl ester (68 mg, 0.1 mmol), **1** (42 mg, 0.12 mmol), and glutathione (307 mg, 1 mmol). Degassed DMSO (3 mL) was added to the reaction vial at room temperature. The vial was then removed from glovebox and stirred at 37 $^\circ\text{C}$ for 8 h. The reaction was monitored by TLC (MeOH/ CHCl_3 1:15 and acetone/hexane 1:5, for the consumption of hemin dimethyl ester and **1**, respectively), and quenched by addition of H_2O (10 mL), extracted by DCM (10 mL \times 2) and EtOAc (10 mL \times 2). The organic layers were combined, washed with brine, and dried over Na_2SO_4 . Column chromatography afforded furanone **38** as the major product, along with a mixture of three paramagnetic, colored,

hemin-containing products, potentially as the regioisomers of Fe(III)-PPIX adduct **39**: HRMS (ESI) calcd. for $[\text{C}_{56}\text{H}_{62}\text{FeN}_4\text{O}_8]^+ (\text{M}-\text{Cl})^+$: m/z 974.3918, found 974.3963.

4.3 In-vitro drug susceptibility of Cardamom Peroxide

4.3.1. Culture-adaptation and maintenance of *P. falciparum*—All parasite samples were collected from patients in Cambodia under protocols approved by Cambodia's National Ethics Committee for Health Research, and the National Institute of Allergy and Infectious Diseases (NIAID) institutional review board (NIH). All protocol subjects provided written informed consent. Culture-adaptation of parasites was accomplished by thawing cryopreserved material containing infected red blood cells (iRBCs) that had been mixed with glycerolyte. Parasites were maintained in fresh human blood (O+) and Hepes buffered RPMI media containing 10% O+ human serum (heat inactivated and pooled). Cultures were placed in modular incubators and gassed with 5% O₂/5% CO₂/balance N₂ gas and incubated in a 37 °C incubator.

4.3.2. Antimalarial drug preparation—Stock solutions of cardamom peroxide were prepared in DMSO. Two-fold serial dilutions of stock solutions were prepared in culture water. Final drug concentrations ranged from 19.5 – 20,000 nM. Fifty µl of each diluted drug solution were added in duplicate to 96-well, flat-bottomed plates (Costar 3595, Corning, Lowell, MA). The drug-coated plates were prepared freshly before use. The quality of each batch of plates was validated by measuring the antimalarial drug responses of the *P. falciparum* 3D7 line.

4.3.3. In-vitro drug susceptibility assay—In-vitro drug susceptibility was measured using the SYBR Green I method as previously described (see: Bacon, D. J.; Latour, C.; Lucas, C.; Colina, O.; Ringwald, P.; Picot, S. *Antimicrob. Agents Chemother.* **2007**, 51, 1172–1178.). Briefly, synchronized rings were grown in the presence of different concentrations of drugs in duplicate wells of drug-coated, clear-bottom, 96-well plates (Costar 3595, Corning, Lowell, MA), at 1% hematocrit, 1% starting parasitemia and 200 µl of 0.5% Albumax culture media. Each plate included two drug-free wells as negative controls for each drug. Plates were placed in a vacuum chamber and gassed with 5% O₂/5% CO₂/balance N₂ gas and incubated in a 37 °C incubator for 72 hours, and subsequently frozen and kept at –20 °C until the measurement of SYBR Green. Growth at 72 hours was measured by SYBR Green I (Invitrogen) staining of parasite DNA. Relative Fluorescence Units (RFU) was measured at an excitation of 485nm and emission of 530nm on a FLUOstar OPTIMA instrument (BMG Labtech, Cary, NC) and analyzed using World Wide Antimalarial Resistance Network (WWARN) IVART analysis (<http://www.wwarn.org/tools-resources/toolkit/analyse/ivart>). The IC₅₀, defined as the drug concentration at which the SYBR Green I signal was 50% of that measured from drug-free control wells, was calculated from IVART software to fit the concentration-inhibition data (see: Woodrow, C. J. *et al. Antimicrob. Agents Chemother.* **2013**, 57, 3121–3130).

4.4 X-ray crystallographic data

Crystallographic data for structures **1**, **3**, **37**, and **38** have been deposited with the Cambridge Crystallographic Data Centre. Copies of the data can be obtained free of charge from <http://>

www.cdc.cam.ac.uk/products/csd/request/ (CDCC #1003088 for **1**, #1003087 for **3**, #1003085 for **37**, and #1003086 for **38**).

Supplementary Material

Refer to Web version on PubMed Central for supplementary material.

Acknowledgments

Financial support is provided by the NIH (GM116952 to T. J. M.). T.J.M. is a Cottrell Scholar and acknowledges unrestricted support from Novartis, Bristol-Myers Squibb, Amgen, and Eli Lilly. X. H. thanks Bristol-Myers Squibb and Amgen for graduate fellowships. We are grateful to Dr. Hasan Celik for NMR assistance wherein NIH grant GM68933 is acknowledged. Dr. Antonio Dipasquale is acknowledged for X-ray crystallographic analysis wherein support from NIH Shared Instrument Grant (S10-RR027172) is also acknowledged. This work was partly supported by the Intramural Research Program of the NIAID, NIH.

References and notes

1. World Health Organization. World Malaria Report. World Health Organization; Geneva, Switzerland: 2017.
2. Rosenthal PJ. Antimalarial Chemotherapy: Mechanisms of Action, Resistance, and New Directions in Drug Discovery. Humana Press; Totowa, NJ: 2011.
3. Poser CM, Bruyn GW. An Illustrated History of Malaria. the Parthenon Publishing Group; Carnforth, UK: 1999.
4. (a) Wellems TE, Plowe CV. *J Infect Dis.* 2001; 184:770–776. [PubMed: 11517439] (b) Hastings IM. *Trends Parasitol.* 2004; 20:512–518. [PubMed: 15471702] (c) Ginsburg H. *Acta Tropica.* 2005; 96:16–23. [PubMed: 16054105]
5. (a) Liu JM, Ni MY, Fen JF, Tu YY, Wu ZH, Wu YL, Zhou WS. *Huaxue Xuebao.* 1979; 37:129–143. (b) Tu Y. *Angew Chem Int Ed.* 2016; 55:10210–10226.
6. (a) Dondorp AM, et al. *Engl J Med.* 2009; 361:455–467. (b) Ashley EA, et al. *New Engl J Med.* 2014; 371:411–423. [PubMed: 25075834] (c) Imwong M, et al. *Lancet Infect Dis.* 2017; 17:491–497. [PubMed: 28161569] (d) Imwong M, Hien TT, Thuy-Nhien NT, Dondorp AM, White NJ. *Lancet Infect Dis.* 2017; 17:1022–1023. [PubMed: 28948924] (e) Rossi G, De Smet M, Khim N, Kindermans JM, Menard D. *Lancet Infect Dis.* 2017; 17:1233. [PubMed: 29173875] (f) Lu F, et al. *N Engl J Med.* 2017; 376:991–993. [PubMed: 28225668]
7. (a) Spitteller G. *Free Radic Biol Med.* 2006; 41:362. [PubMed: 16843819] (b) Dembitsky VM, Glorizova TA, Poroikov VV. *Mini Rev Med Chem.* 2007; 7:571. [PubMed: 17584156] (c) Chaturvedi D, Goswami A, Saikia PP, Barua NC, Rao PG. *Chem Soc Rev.* 2010; 39:435. [PubMed: 20111769] (d) Schwikard S, van Heerden FR. *Nat Prod Rep.* 2002; 19:675–692. [PubMed: 12521264] (e) Kaur M, Jain M, Kaur T, Jain R. *Bioorg Med Chem Lett.* 2009; 17:3229–3256. (f) Dembitsky VM. *J Mol Genet Med.* 2015; 9:163.
8. For total syntheses of the structures shown in Figure 1A, see: Schmid G, Hofheinz W. *J Am Chem Soc.* 1983; 105:624–625. Xu XX, Zhu J, Huang DZ, Zhou WS. *Tetrahedron.* 1986; 42:819–828. Avery MA, Chong WKM, White CJ. *J Am Chem Soc.* 1992; 114:974–979. Avery MA, White CJ, Chong WKM. *Tetrahedron Lett.* 1987; 28:4629–4632. Liu HJ, Yeh WL, Chew S Y. *Tetrahedron Lett.* 1993; 34:4435–4438. Constantino MG, Beltrame M Jr, da Silva GVJ. *Synth Commun.* 1996; 26:321–329. Yadav JS, Babu RS, Sabitha G. *Tetrahedron Lett.* 2003; 44:387–389. Yadav JS, Thirupathiah B, Srihari P. *Tetrahedron.* 2010; 66:2005–2009. Zhou WS, Xu XX. *Acc Chem Res.* 1994; 27:211–216. Zhu C, Cook SP. *J Am Chem Soc.* 2014; 134:13577–13579. Hilf JA, Witthoft LW, Woerpel KA. *J Org Chem.* 2015; 80:8262–8267. [PubMed: 26158427] Xu XX, Dong HQ. *Tetrahedron Lett.* 1994; 35:9429–9432. Szpilman AM, Korshin EE, Rozenberg H, Bachi MD. *J Org Chem.* 2005; 70:3618–3632. [PubMed: 15844999] Xu XX, Zhu J, Huang DZ, Zhou WS. *Tetrahedron Lett.* 1991; 32:5785–5788. Li Q, Zhao K, Peuronen A, Rissanen K, Enders D, Tang YJ. *Am Chem Soc.* 2018; just accepted. doi: 10.1021/jacs.7b12903

9. For reviews on the synthesis of endoperoxides, see: Korshin EE, Bachi MD. Synthesis of Cyclic Peroxides. Patai's Chemistry of Functional Groups, Online. Wiley 2009:1–117. Dussault P. Synlett. 1995:997.
10. (a) Slack RD, Jacobine AM, Posner GH. Med Chem Commun. 2012; 3:281–297. (b) Schlitzer M. ChemMedChem. 2007; 2:944–986. [PubMed: 17530725] (c) Hofheinz W, Burgin H, Gocke E, Jaquet C, Masciadri R, Schmid G, Stohler H, Urwyler H. Trop Med Parasitol. 1994; 45:261–265. (d) Vennerstrom JL, et al. Nature. 2004; 430:900–904. [PubMed: 15318224]
11. For recent examples of non-peroxidic antimalarials, see: Flannery EL, Chatterjee AK, Winzeler EA. Nat Rev Microbiol. 2013; 11:849–862. [PubMed: 24217412] Baragana B, et al. Nature. 2015; 522:315–320. [PubMed: 26085270] Kato N, Comer E, Sakata-Kato T, Sharma A, Sharma M, Maetani M, Bastien J, Brancucci NM, Bittker JA, Corey V, Clarke D, Derbyshire ER, Dornan GL, Duffy S, Eckley S, Itoe MA, Koolen KM, Lewis TA, Lui PS, Lukens AK, Lund E, March S, Meibalan E, Meier BC, McPhail JA, Mitasev B, Moss EL, Sayes M, Van Gessel Y, Wawer MJ, Yoshinaga T, Zeeman AM, Avery VM, Bhatia SN, Burke JE, Catteruccia F, Clardy JC, Clemons PA, Dechering KJ, Duvall JR, Foley MA, Gusovsky F, Kocken CH, Marti M, Morningstar ML, Munoz B, Neafsey DE, Sharma A, Winzeler EA, Wirth DF, Scherer CA, Schreiber SL. Nature. 2016; 538:344–349. [PubMed: 27602946] Cowell AN, et al. Science. 2018; 359:191–199. [PubMed: 29326268]
12. Kamchonwongpaisan S, Nilanonta C, Tarnchompoo B, Thebtaranonth C, Thebtaranonth Y, Yuthavong Y, Kongsaree P, Clardy J. Tetrahedron Lett. 1995; 36:1821–1824.
13. Hu X, Maimone TJ. J Am Chem Soc. 2014; 136:5287–5290. [PubMed: 24673099]
14. Czechowski T, Larson TR, Catania TM, Harvey D, Brown GD, Graham IA. Proc Natl Acad Sci. 2016; 113:15150–15155. [PubMed: 27930305]
15. Cointeaux L, Berrien JF, Mayrargue J. Tetrahedron Lett. 2002; 43:6275–6277.
16. Brill ZG, Condakes ML, Ting CP, Maimone TJ. Chem Rev. 2017; 117:11753–11795. [PubMed: 28293944]
17. Mazzega M, Fabris F, Cossu S, De Lucchi O, Lucchini V, Valle G. Tetrahedron. 1999; 55:4427–4440.
18. Willis MC. Chem Rev. 2010; 110:725–748. [PubMed: 19873977]
19. Nicolaou KC, Ellery SP, Chen JS. Angew Chem Int Ed. 2009; 48:7140–7165.
20. Barrero AF, Herrador MM, del Moral JF, Arteaga P, Arteaga JF, Dieguez HR, Sanchez EM. J Org Chem. 2007; 72:2988–2995. [PubMed: 17375959]
21. Lipshutz BH, Hackmann C. J Org Chem. 1994; 59:7437–7444.
22. Dutta DK, Konwar D. Tetrahedron Lett. 2000; 41:6227–6229.
23. Baati R, Mioskowski C, Barma D, Kache R, Falck JR. Org Lett. 2006; 8:2949–2951. [PubMed: 16805524]
24. Furstner A, Hupperts A. J Am Chem Soc. 1995; 117:4468–4475.
25. Dieguez HR, Lopez A, Domingo V, Arteaga JF, Dobado JA, Herrador MM, Quilez del Moral JF, Barrero AF. J Am Chem Soc. 2010; 132:254–259. [PubMed: 20000601]
26. Mukaiyama T, Sato T, Hanna J. Chem Lett. 1973:1041–1044.
27. (a) McMurry JE, Fleming MP, Kees KL, Krepski LR. J Org Chem. 1978; 43:3255–3266. (b) McMurry JE. Chem Rev. 1989; 89:1513–1524.
28. Kornblum N, Delamare HE. J Am Chem Soc. 1951; 73:880–881.
29. Yaremenko IA, Vil' VA, Demchuk DV, Terent'ev AO. Beilstein J Org Chem. 2016; 12:1647–1748. [PubMed: 27559418]
30. (a) Nokami J, Nishimura A, Sunami M, Wakabayashi S. Tetrahedron Lett. 1987; 28:649–650. (b) Atasoy B, Balci M. Tetrahedron. 1986; 42:1461–1468.
31. Gersmann HR, Bickel AF, Nieuwenhuis HJW. Proc Chem Soc. 1962:279.
32. Novkovic L, Trmcic M, Rodic M, Bihelovic F, Zlatar M, Matovic R, Saicic RN. Rsc Advances. 2015; 5:99577–99584.
33. Chumoyer MY, Danishefsky SJ. J Am Chem Soc. 1992; 114:8333–8334.
34. Magnus P, Booth J, Magnus N, Tarrant J, Thom S, Ujjainwalla F. Tetrahedron Lett. 1995; 36:5331–5334.

35. Nickel A, Maruyama T, Tang H, Murphy PD, Greene B, Yusuff N, Wood JL. *J Am Chem Soc.* 2004; 126:16300–16301. [PubMed: 15600313]
36. Schottner E, Wiechoczek M, Jones PG, Lindel T. *Org Lett.* 2010; 12:784–787. [PubMed: 20085310]
37. Gampe CM, Carreira EM. *Angew Chem Int Ed.* 2011; 50:2962–2965.
38. House HO, Ro RS. *J Am Chem Soc.* 1958; 80:2428–2433.
39. Greatrex BW, Jenkins NF, Taylor DK, Tiekink ER. *J Org Chem.* 2003; 68:5205–5210. [PubMed: 12816478]
40. Crossley SWM, Obradors C, Martinez RM, Shenvi RA. *Chem Rev.* 2016; 116:8912–9000. [PubMed: 27461578]
41. (a) Mukaiyama T, Isayama S, Inoki S, Kato K, Yamada T, Takai T. *Chem Lett.* 1989:449–452. (b) Inoki S, Kato K, Takai T, Isayama S, Yamada T, Mukaiyama T. *Chem Lett.* 1989:515–518. (c) Isayama S, Mukaiyama T. *Chem Lett.* 1989:1071–1074. (d) Isayama S. *Bull Chem Soc Jpn.* 1990; 63:1305–1310.
42. Inoki S, Kato K, Isayama S, Mukaiyama T. *Chem Lett.* 1990:1869–1872.
43. Magnus and coworkers repeated the synthetic procedure to prepare $Mn(dpm)_2$ in air, but the obtained product was identified as $Mn(dpm)_3$. The structure of $Mn(dpm)_3$ was determined by X-Ray analysis. (See references 43–46)
44. Magnus P, Payne AH, Waring MJ, Scott DA, Lynch V. *Tetrahedron Lett.* 2000; 41:9725–9730.
45. Magnus P, Scott DA, Fielding MR. *Tetrahedron Lett.* 2001; 42:4127–4129.
46. Magnus P, Waring MJ, Scott DA. *Tetrahedron Lett.* 2000; 41:9731–9733.
47. Magnus P, Fielding MR. *Tetrahedron Lett.* 2001; 42:6633–6636.
48. (a) Iwasaki K, Wan KK, Oppedisano A, Crossley SW, Shenvi RA. *J Am Chem Soc.* 2014; 136:1300–1303. [PubMed: 24428640] (b) Obradors C, Martinez RM, Shenvi RA. *J Am Chem Soc.* 2016; 138:4962–4971. [PubMed: 26984323] (c) King SM, Ma X, Herzon SB. *J Am Chem Soc.* 2014; 136:6884. [PubMed: 24824195] (d) Ma X, Herzon SB. *Chem Sci.* 2015; 6:6250. [PubMed: 30090243]
49. For mechanistically related hydrofunctionalization methodology, see: Waser J, Carreira EM. *J Am Chem Soc.* 2004; 126:5676. [PubMed: 15125654] Waser J, Carreira EM. *Angew Chem Int Ed.* 2004; 43:4099. Waser J, Nambu H, Carreira EM. *J Am Chem Soc.* 2005; 127:8294. [PubMed: 15941257] Waser J, Gaspar B, Nambu H, Carreira EM. *J Am Chem Soc.* 2006; 128:11693. [PubMed: 16939295] Gaspar B, Carreira EM. *Angew Chem Int Ed.* 2007; 46:4519. Gaspar B, Carreira EM. *Angew Chem Int Ed.* 2008; 120:5842. Gaspar B, Carreira EM. *J Am Chem Soc.* 2009; 131:13214. [PubMed: 19715273] Barker TJ, Boger DL. *J Am Chem Soc.* 2012; 134:13588. [PubMed: 22860624] Tokuyasu T, Kunikawa S, Masuyama A, Nojima M. *Org Lett.* 2002; 4:3595. [PubMed: 12375896] Shigehisa H, Aoki T, Yamaguchi S, Shimizu N, Hiroya K. *J Am Chem Soc.* 2013; 135:10306. [PubMed: 23819774] Hashimoto T, Hirose D, Taniguchi T. *Angew Chem Int Ed.* 2014; 53:2730. Ma X, Herzon SB. *J Org Chem.* 2016; 81:8673. [PubMed: 27598718] Ma X, Herzon SB. *J Am Chem Soc.* 2016; 138:8718. [PubMed: 27384921] Ma X, Dang H, Rose JA, Rablen P, Herzon SB. *J Am Chem Soc.* 2017; 139:5998. [PubMed: 28359149]
50. Sugimori T, Horike S, Tsumura S, Handa M, Kasuga K. *Inorg Chim Acta.* 1998; 283:275–278.
51. Leggans EK, Barker TJ, Duncan KK, Boger DL. *Org Lett.* 2012; 14:1428–1431. [PubMed: 22369097]
52. Sears JE, Boger DL. *Acc Chem Res.* 2015; 48:653–662. [PubMed: 25586069]
53. (a) Lo JC, Yabe Y, Baran PS. *J Am Chem Soc.* 2014; 136:1304–1307. [PubMed: 24428607] (b) Lo JC, Gui J, Yabe Y, Pan CM, Baran PS. *Nature.* 2014; 516:343–348. [PubMed: 25519131] (c) Gui J, Pan CM, Jin Y, Qin T, Lo JC, Lee BJ, Spengel SH, Mertzman ME, Pitts WJ, La Cruz TE, Schmidt MA, Darvatkar N, Natarajan SR, Baran PS. *Science.* 2015; 348:886–891. [PubMed: 25999503] (d) Dao HT, Li C, Michaudel Q, Maxwell BD, Baran PS. *J Am Chem Soc.* 2015; 137:8046–8049. [PubMed: 26088401]
54. Gu X, Zhang W, Salomon RG. *J Org Chem.* 2012; 77:1554–1559. [PubMed: 22204279]
55. A direct Hock-Criegee-type fragmentation of 25 could also ultimately lead to nopinone and diketone 30, see reference 29.
56. Michon C, Djukic JP, Ratkovic Z, Pfeffer M. *Tetrahedron Lett.* 2002; 43:5241–5243.

57. (a) Golenser J, Waknine JH, Krugliak M, Hunt NH, Grau GE. *Int J Parasitol.* 2006; 36:1427. [PubMed: 17005183] (b) O'Neill PM, Barton VE, Ward SA. *Molecules.* 2010; 15:1705. [PubMed: 20336009] (c) Posner GH, O'Neill PM. *Acc Chem Res.* 2004; 37:397. [PubMed: 15196049]
58. Posner GH, Cumming JN, Ploypradith P, Chang HO. *J Am Chem Soc.* 1995; 117:5885–5886.
59. Wu WM, Wu Y, Wu YL, Yao ZJ, Zhou CM, Li Y, Shan F. *J Am Chem Soc.* 1998; 120:3316–3325.
60. Robert A, Cazelles J, Meunier B. *Angew Chem Int Ed.* 2001; 40:1954–1957.
61. Robert A, Coppel Y, Meunier B. *Chem Commun.* 2002:414–415.
62. For selected examples, see: Posner GH, O'Neill PM. *Acc Chem Res.* 2004; 37:397–404. [PubMed: 15196049] Wu WM, Wu Y, Wu YL, Yao ZJ, Zhou CM, Li Y, Shan F. *J Am Chem Soc.* 1998; 120:3316–3325. O'Neill PM, Stocks PA, Pugh MD, Araujo NC, Korshin EE, Bickley JF, Ward SA, Bray PG, Pasini E, Davies J, Verissimo E, Bachi MD. *Angew Chem, Int Ed.* 2004; 43:4193–4197. Tang Y, Dong Y, Wang X, Sriraghavan K, Wood JK, Vennerstrom JL. *J Org Chem.* 2005; 70:5103–5110. [PubMed: 15960511]
63. Weissbuch I, Leiserowitz L. *Chem Rev.* 2008; 108:4899–4914. [PubMed: 19006402]
64. Lim P, et al. *Antimicrob Agents Chemother.* 2013; 57:5277–5283. [PubMed: 23939897]
65. This is possibly a result of mutations which increase the ability of the parasite to manage oxidative damage. For a recent discussion, see: Paloque L, Ramadan AP, Mercereau-Puijalon O, Augereau JM, Benoit-Vical F. *Malaria J.* 2016; 15:149.
66. For recent studies on artemisinin resistance, see: Straimer J, et al. *Science.* 2015; 347:6220. Ariey F, et al. *Nature.* 2014; 505:50–55. [PubMed: 24352242] Mbengue A, et al. *Nature.* 2015; 520:683. [PubMed: 25874676]
67. (a) Saicic RN. *Tetrahedron.* 2014; 70:8183–8218. (b) Young IS, Baran PS. *Nat Chem.* 2009; 1:193–205. [PubMed: 21378848]

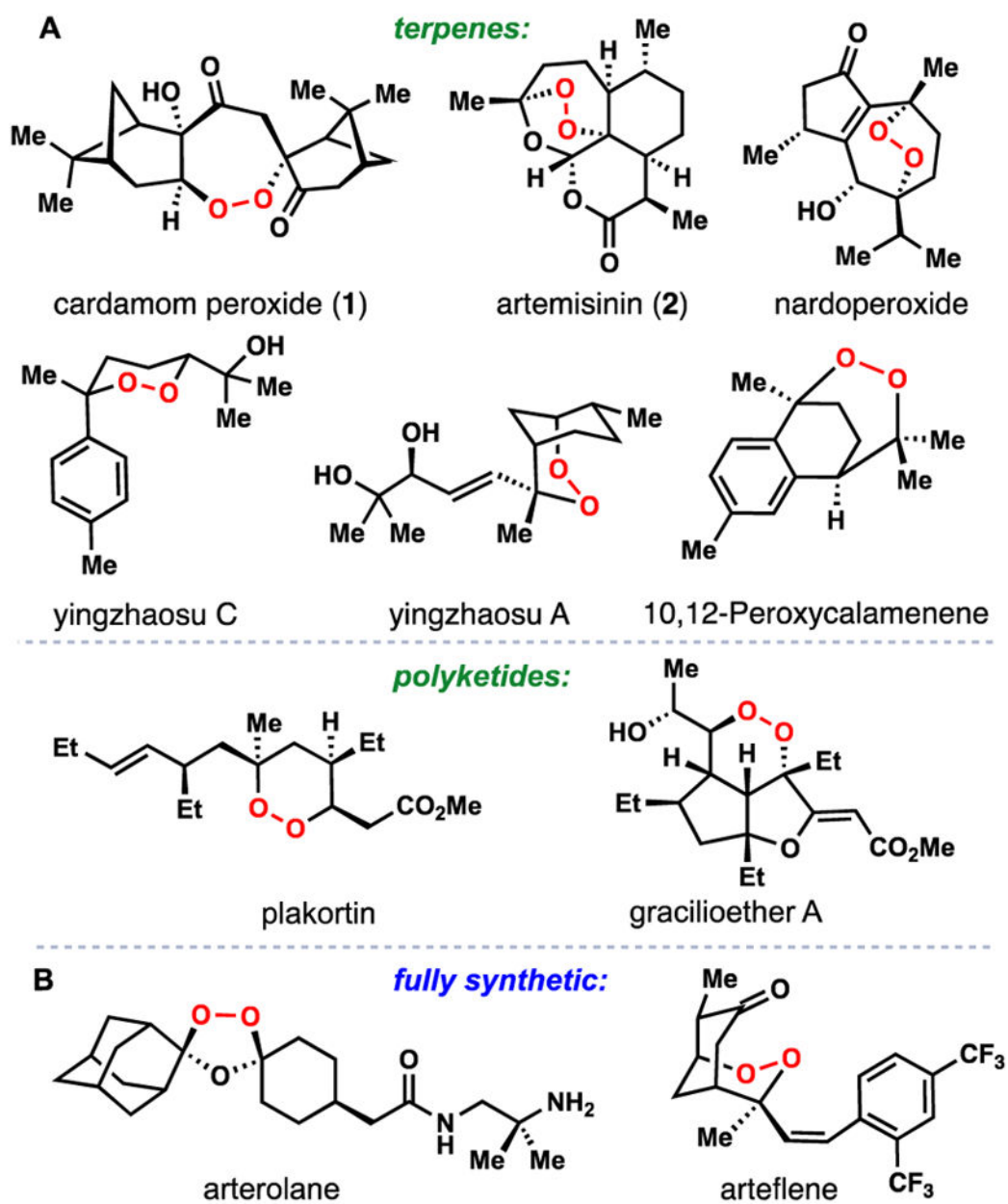


Figure 1. Antimalarials containing an oxygen-oxygen bond. **A)** selected endoperoxide-containing natural products. **B)** fully synthetic molecules inspired by natural products.

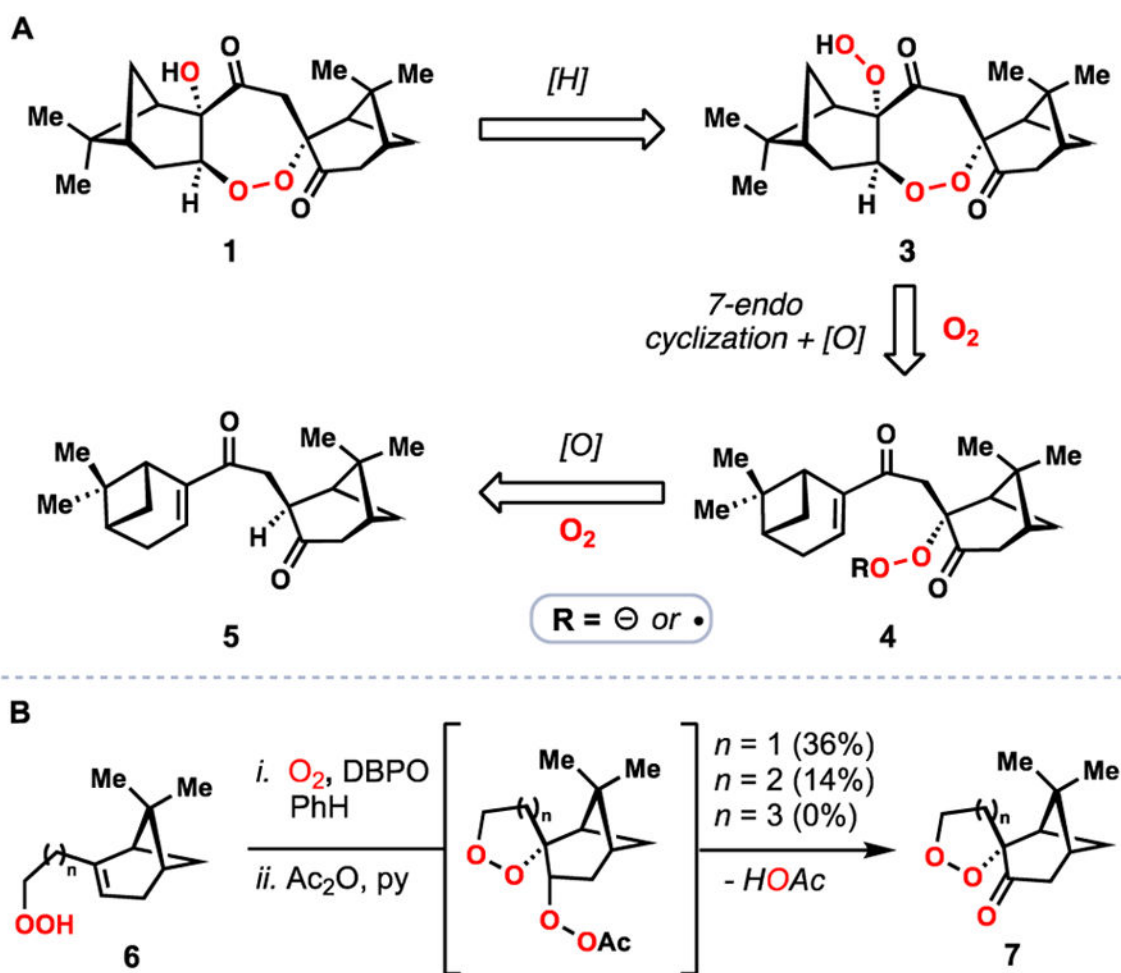


Figure 2. Synthetic approaches to **1**. **A)** initial retrosynthesis. **B)** studies by Mayrargue and co-workers demonstrates the challenge in forming the 1,2-dioxepane unit found in **1**. (DBPO = Di-*tert*-butyl peroxyoxalate)

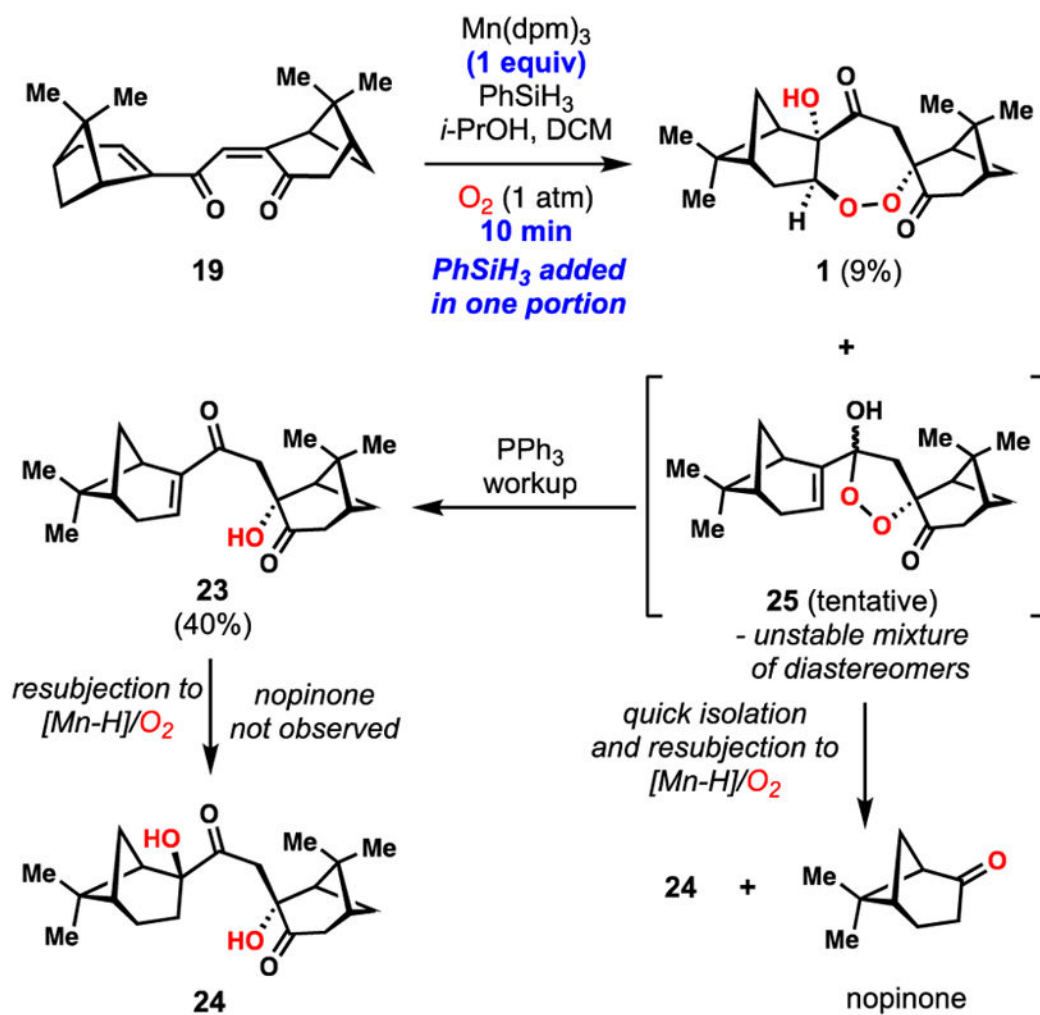


Figure 3. Investigation into the formation of side-products during the polyoxygenation cascade.

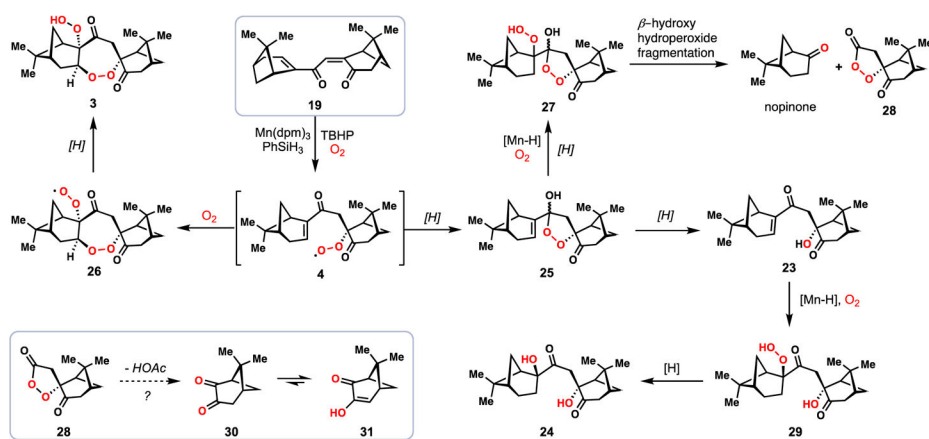


Figure 4.
Potential mechanism for the polyoxygenation cascade.

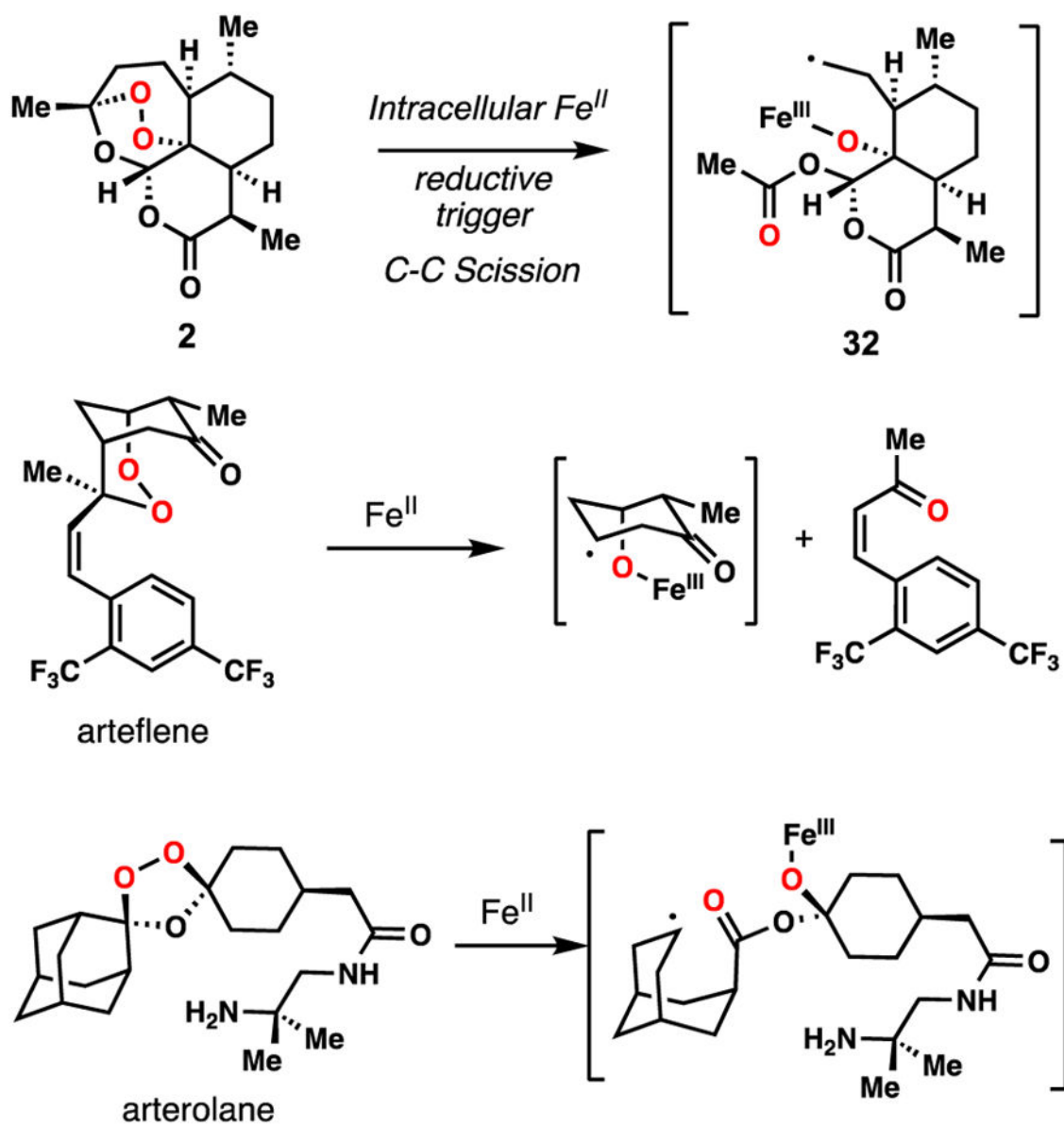


Figure 5. Selected, characterized activation modes of various O–O bond-containing antimalarials in the presence of Fe^{II}

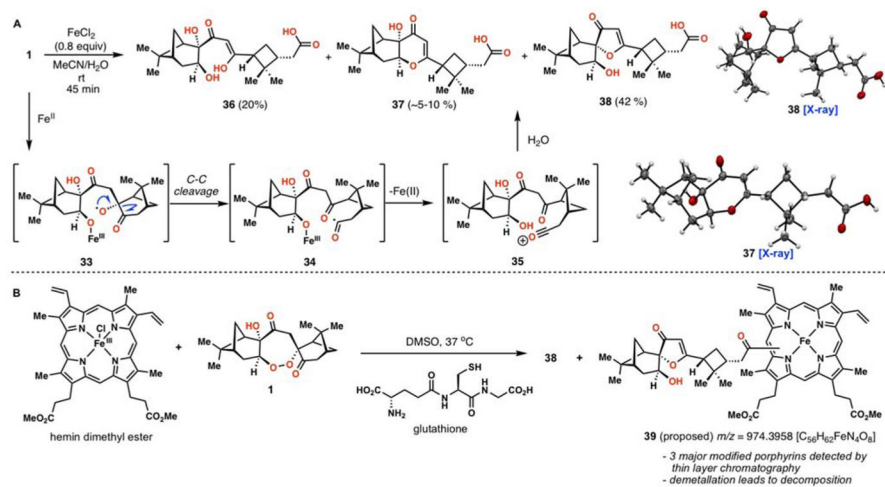


Figure 6.
Activation modes of **1** in the presence of various Fe^{II} sources.

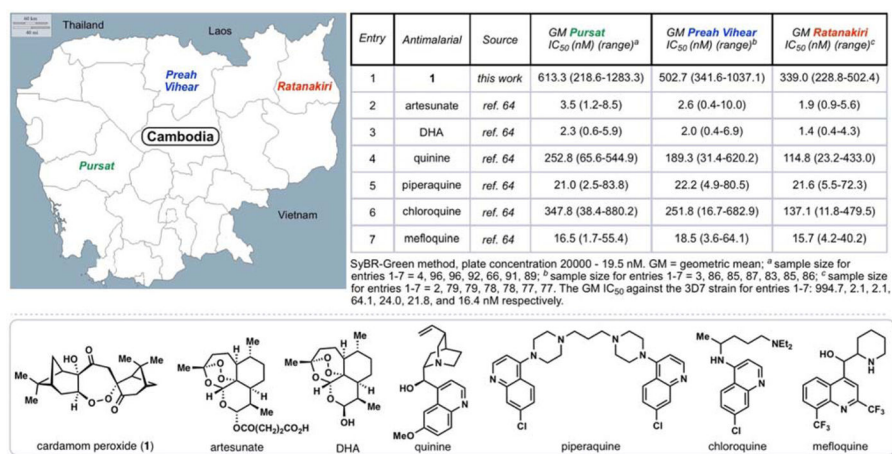
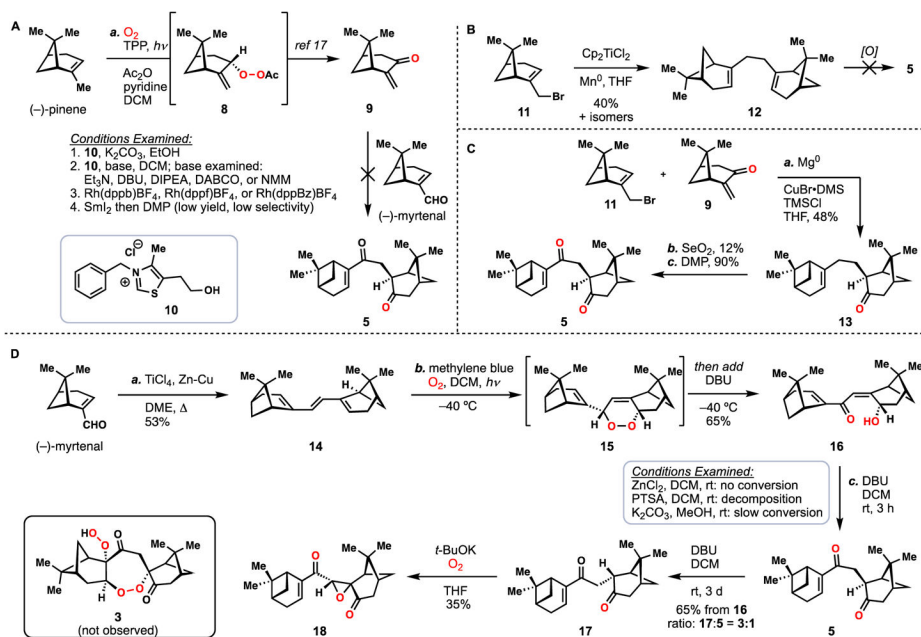
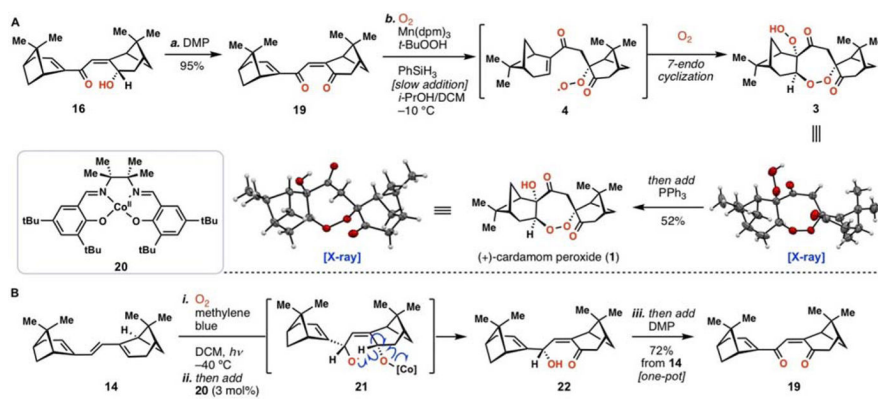


Figure 7. Antimalarial activity of **1** against *P. falciparum* clinical field isolates from three provinces of Cambodia.

**Scheme 1.**

Synthesis of dimer **5** and failed conversion to **3**. **A)** Unsuccessful Stetter approach to **5**. **B)** Unproductive reductive coupling strategy. **C)** Successful synthesis of **5**. **D)** Improved synthesis of **5** and failed conversion to **3**.

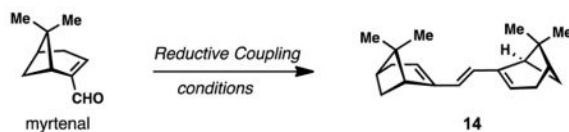
**Scheme 2.**

Total synthesis of the cardamom peroxide. **A**) Successful radical-based oxygenation cascade.

B) One-pot synthesis of **19** from **14**.

Table 1

(-)-Myrtenal reductive coupling: selected optimization.



Entries/Conditions ^a	Yield %
1 AlCl ₃ (2 equiv), Zn (2 equiv), MeCN (0.1 M)	0
2 CrCl ₂ (4 equiv), HSiCl ₃ (5 equiv), THF (0.07 M)	0
3 Ti ⁰ (30 equiv), TMSCl (30 equiv), DME (0.07 M)	<10 ^b
4 Cp ₂ TiCl ₂ (1.2 equiv), Mn (2.4 equiv), THF (0.1 M)	17 ^b
5 Cp ₂ TiCl ₂ (1.2 equiv), Zn (2.4 equiv), THF (0.1 M) 6 Cp ₂ TiCl ₂ (0.3 equiv), TMSCl (4 equiv), Mn (8 equiv), THF (0.1 M)	18 ^b
7 TiCl ₄ (1.2 equiv), Zn (2.4 equiv), THF (0.1 M)	0
8 TiCl ₃ (11 equiv), Zn-Cu (30 equiv), DME (0.01 M)	35 ^b
9 TiCl ₄ (10 equiv), Zn-Cu (40 equiv), DME (0.01 M)	51 ^{c,d}
	62 ^{c,d,e}

^aReaction performed on a 0.1 g scale, conditions detailed in references unless otherwise stated.

^bNMR yield, with dibromomethane as internal standard.

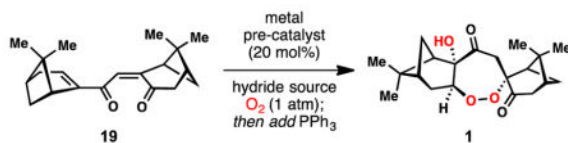
^cIsolated yield.

^dMyrtenal was added in two portions over 24 h.

^eReaction afforded 53 % of **14** on a 3g scale. Cp = cyclopentadienyl, DME = 1,2-dimethoxyethane, THF = tetrahydrofuran.

Table 2

Optimization of the tandem peroxidation reaction.



Entries/Conditions ^a	Yield %
1 Fe ₂ (ox) ₃ ·6H ₂ O (5.0 equiv), NaBH ₄ (6.4 equiv), EtOH/H ₂ O, 0 °C	0
2 Fe ^{II} (Pc), NaBH ₄ (3.0 equiv), EtOH, 0 °C	0
3 Fe(acac) ₃ , PhSiH ₃ (2.5 equiv), EtOH, 0 °C to rt	0
4 Co(acac) ₂ , PhSiH ₃ (2.5 equiv), DCM/ <i>i</i> -PrOH, -10 °C to rt	6
5 Mn(dpm) ₃ , PhSiH ₃ (2.5 equiv), DCM/ <i>i</i> -PrOH, -10 °C	34
6 Mn(dpm) ₃ , PhSiH ₃ (2.5 equiv), DCM/ <i>i</i> -PrOH, -10 °C	41 ^b
7 Mn(dpm) ₃ , PhSiH ₃ (2.5 equiv), <i>t</i> -BuOOH (1.5 equiv), DCM/ <i>i</i> -PrOH, -10 °C	52 ^b

^aReaction performed on a 0.1 mmol scale using 20 mol % of metal catalyst unless otherwise stated.

^bPhSiH₃ added slowly over 12 h as a solution in DCM. Pc = Phthalocyanine, ox = oxalate, acac = acetylacetonate, dpm = dipivaloylmethanato.

